Energy Economics 140 (2024) 107987

Contents lists available at ScienceDirect

Energy Economics

journal homepage: www.elsevier.com/locate/eneeco

Dynamic connectedness in the higher moments between clean energy and oil prices

Wei Hao [a,*], Linh Pham [b]

[a] School of Economics and Finance, Massey University, Wallace Street, Mount Cook, Wellington 6021, New Zealand
[b] Economics, Business and Finance Department, Lake Forest College Lake Forest, IL 60045, USA

ARTICLE INFO

JEL classifications:
G10
G11
Q4

Keywords:
Clean energy
Oil
Higher-order moment spillovers
Higher-order moment portfolio strategies

ABSTRACT

Focusing on clean energy stocks and oil prices, we find that connectedness between these assets not only exists in volatility, but also at higher-order moments, such as skewness and kurtosis, which have been largely under studied in the existing literature. Estimating the connectedness using intra-day data, our initial static analyses suggest that the connectedness between the clean energy and oil markets is heterogenous across the moments and the shock transmitter/recipient role played by each market varies across moments. Further dynamic analyses indicate that higher-order moment connectedness is also time varying and appears to be stronger during uncertain market conditions. In addition, we identify day-of-the-week patterns of higher-order moment connectedness during high uncertainty periods, but these patterns appear to be reversed during low uncertainty periods. The employment of Markov switching regression models further corroborates the market uncertainties as the determinants of higher-order moment connectedness. As an important extension, we provide empirical evidence that including clean energy stocks in the investment portfolio can effectively hedge oil price risks and considering higher-order moments in constructing investment strategies adds extra value to investors. Our utility-based hedging strategy and minimum connectedness portfolio can offer higher utility gains and better risk-return trade-offs to those investors who are not infinitely risk-averse.

1. Introduction

Since the early 2000s, the clean energy market has witnessed tremendous growth thanks to increasing interest among investors, policymakers, and the public in reducing climate risks and promoting a climate-resilient economy. Since 2004, global energy transition investment has witnessed an increasing trend that remained strong throughout the most recent crises including the global financial crisis and the COVID-19 pandemic. In 2022, global energy transition investment totaled $1.1 trillion representing an increase of 31 % compared to the previous year (Bloomberg New Energy Finance, 2023). Despite the fast growth in clean energy investments, fossil fuels remain a main source of energy. In 2021, 13.47 % of global primary energy came from renewable technologies.[1]

Moreover, as a substitute for fossil fuel energy, the performance of clean energy stock markets depends largely on movement in oil prices. The literature has provided a wide range of empirical evidence on the relationship between clean energy stock markets and oil prices (Henriques and Sadorsky, 2008; Managi and Okimoto, 2013; Kocaarslan and Soytas, 2019; Yahya et al., 2021; Hammoudeh et al., 2021; Tiwari et al., 2023). These previous studies have extensively studied the relationship between the clean energy and oil markets. However, they have focused on documenting the clean energy-oil price relationship in either returns or volatility using daily data, while little empirical evidence has existed on the relationship at higher-order moments. Since asset returns typically demonstrate non-normal, asymmetric, and fat-tailed distribution in the real world, it is highly relevant and important to consider higher-order moments of asset return distribution beyond just return and volatility (Bouri et al., 2021). Modeling the dynamic connectedness structure between clean energy and oil prices at higher-order moments can offer additional valuable information to guide investors and portfolio managers in constructing optimal portfolios. This, in turn, facilitates the investment flows toward green economic activities and a better transition to a climate-resilient economy. Against this background, the objectives of this paper are as follows. First, we estimate the higher-order moments, specifically, realized volatility, the jump component

* Corresponding author.
E-mail address: w.hao@massey.ac.nz (W. Hao).

[1] https://ourworldindata.org/renewable-energy

https://doi.org/10.1016/j.eneco.2024.107987
Received 6 November 2023; Received in revised form 6 October 2024; Accepted 12 October 2024
Available online 24 October 2024

of realized volatility, realized skewness, and realized kurtosis, for the clean energy and oil markets. In addition, we examine the spillover effects among clean energy stock markets and oil prices at higher-order moments. In doing so, we are able to unveil unique characteristics of the clean energy-oil linkages that are not captured by the first moments (e.g., volatility, jump, asymmetry, and fat tail risk spillovers). This allows us to quantify the spillovers of specific risks, such as downside or tail risks. Moreover, we identify the roles of financial and macroeconomic uncertainty on the higher-order moment spillovers by identifying the spillover patterns across low and high uncertainty states. Finally, we derive the economic and financial implications of our results for investors and policymakers.

To achieve the above objectives, we collect intra-day data at the five-minute frequency on oil prices and various clean energy subsector indexes from October 2010–November 2022. Specifically, we consider the NASDAQ OMX Biofuel, Wind, Solar, Renewable Energy Generation, and Energy Efficiency Indexes. Based on the intra-day data, we calculate the realized variance and its jump component, realized skewness and realized kurtosis of each variable following Andersen and Bollerslev (1998), Barndorff-Nielsen et al. (2010) and Corsi et al. (2010). Next, we study the links between the clean energy and oil markets using Balcilar et al.'s (2021) time-varying parameter (TVP) extended joint connectedness model. Then, we analyze the day-of-the week pattern of the connectedness across the markets and employ a Markov-switching regression model to investigate how this connectedness varies across different states. Finally, we demonstrate the usefulness of higher-order moments in portfolio management.[2] Compared to other approaches, such as quantile regressions or copulas, our model offers several advantages. First, we utilize high frequency, intraday data to calculate the realized higher-order moments of clean energy and oil returns. While copula models or quantile analyses, such as the quantile connectedness model, estimate extreme market spillovers using daily data, intraday data contains richer information about market movement (Andersen et al., 2003; Barndorff-Nielsen et al., 2010; Baruník et al., 2015, 2017). Specifically, realized volatility measures the return variations and skewness measures the return asymmetries, while kurtosis measures the thickness of the tails of the return distributions. By analyzing the spillovers across markets at higher-order moments, we seek to quantify specific risk spillovers between the oil and clean energy markets, such as downside risks or tail risks. In addition, the realized measures are semi-nonparametric measures of higher moments that do not depend on underlying assumptions about return distributions. Moreover, our connectedness model allows us to model the connectedness across variables in a multivariate setting. This helps identify the dependence between any pair of assets in the system while controlling for interactions with other assets.

Our connectedness model indicates that the total connectedness index is highest for realized volatility and its jump component, which is approximately three times larger than that of realized skewness and kurtosis. This indicates that realized volatility and jump spillovers are the dominant determinants of the interdependence among the clean energy and oil markets. However, our results also indicate the relevance of analyzing the clean energy-oil relationship in skewness and kurtosis as significant spillovers (i.e., more than 20 %) still exist at these moments. Moreover, the roles of each market in the system vary widely across the moments. For example, oil is a shock transmitter in volatility and its jump component, but becomes a shock receiver in skewness and kurtosis. Clean energy sectors, such as biofuel, renewable energy generation, and energy efficiency sectors, are net shock receivers in volatility, but move toward the shock transmitter roles in skewness and kurtosis. In addition, we identify two clusters of relatively highly connected assets in the system. Specifically, biofuel and oil form their own cluster, while other renewable markets form another cluster. Finally, we find an increase in the connectedness across the markets during the most recent COVID-19 and Russia-Ukraine war crisis.

Next, using paired sample *t*-tests, our results confirm that the connectedness across oil and clean energy markets varies across trading days where the total connectedness indexes are the lowest on Mondays and gradually trend upward throughout the trading week. This can be attributed to the initial lack of new information at the opening of the trading week. In addition, we notice that this pattern is stronger during high uncertainty periods compared to low uncertainty periods suggesting that the connectedness across the oil and clean energy markets significantly depends upon market uncertainty. To further explore this phenomenon, we estimate a Markov-switching model of the total connectedness indexes on various financial and economic uncertainty variables. Our results indicate that oil and stock market uncertainty play a significant role in determining the connectedness across the markets, while economic policy uncertainty and geopolitical risk play a more modest role.

Finally, we present the usefulness of incorporating higher-order moments into asset allocation decisions by considering the performance of alternative hedging strategies. Our results show that higher-order moment connectedness across clean energy and oil returns is significant, and that incorporating higher-order moment connectedness into portfolio management strategies leads to better risk-return tradeoffs (as proxied by information ratio) and higher utility for certain groups of investors depending on their risk preferences.

Our paper contributes to the literature in the following ways. While previous studies focus on the spillover effects in returns and volatility, we focus on the spillovers across the oil and clean energy markets at higher realized moments. Recent empirical studies have shown that connectedness in higher realized moments can reveal meaningful information, particularly when asset returns are not normally distributed (Bonato et al., 2020; Bouri et al., 2021; Zhang et al., 2023; Hanif et al., 2023). Skewness spillovers capture the spread of return asymmetry across markets, while kurtosis spillovers capture the spread of extreme events or fat tail risks across markets. These higher-order-moment spillovers can influence the stability of financial markets raising the need to study them in detail.

Our results provide important implications for both investors and policymakers. First, we provide empirical evidence that including clean energy stocks in an investment portfolio can effectively hedge oil price risks, and considering higher-order moments of asset returns offers better utility and risk-return trade-off to investors. Our findings provide greater incentives for environmentally conscious investors to pursue green investments. In addition, we find that the connectedness between the clean energy and oil markets is moment dependent, and the shock transmitter and recipient roles played by these markets are heterogenous and time varying. Policymakers should consider these unique features in designing policies to tackle energy challenges and to promote a sustainable and greener future.

The remainder of the paper proceeds as follows. Section 2 presents the literature review, while Section 3 describes the data sources and empirical methodology. Section 4 provides the estimation results. Section 5 discusses the economic and financial implications with the empirical evidence, and Section 6 provides our conclusions.

2. Literature review

Our paper relates to the literature regarding the relationship between oil prices and the clean energy stock markets. Early works in this literature employ vector-autoregressive (VAR) and vector error correction model (VECM) approaches to model the clean energy-oil nexus. For example, Henriques and Sadorsky (2008) use a four-variable VAR model and find an insignificant impact of oil price shocks on renewable energy stock prices. Kumar et al. (2012) extend this framework by adding carbon prices as an additional variable and find evidence of a

[2] We present a block diagram in Appendix D to help readers better understand our methodologies.

substitution effect between oil and renewable energy stock prices. Managi and Okimoto (2013) introduce structural breaks to the VAR model and confirm a changing relationship between oil and renewable energy prices before and after the break. Another strand of the literature employs GARCH models to account for the volatility clustering patterns of oil and clean energy stock prices (Broadstock et al., 2012; Sadorsky, 2012; Ahmad et al., 2018; Pham, 2019; Lv et al., 2021). These studies indicate that clean energy stocks are, on average, weakly correlated with oil prices. However, the relationship between clean energy stocks and oil prices varies across clean energy subsectors. Specifically, Pham (2019) finds that biofuel and energy management stocks are the most connected to oil prices, while wind, geothermal, and fuel cell stocks are among the least connected to oil prices.

One disadvantage of the studies discussed above is that they do not capture the relationship between oil prices and clean energy stocks at the tails, which may be relevant for investment decisions during crisis periods, such as a global financial crisis, the recent COVID-19 pandemic, or the Russia-Ukraine war. Using copulas, Reboredo (2015) finds a time-varying and symmetric tail dependence between oil and renewable energy. Tiwari et al. (2021) employ a dependence-switching copula model to examine the tail dependence between oil prices and the stock returns of clean energy and technology companies. They find that the dependence structures across these markets vary between positive and negative correlation regimes. Uddin et al. (2019) employ a cross-quantilogram approach to study the dependence between renewable energy and other assets and determine that renewable energy is positively influenced by oil prices, and this relationship dissipates in the long run. Tiwari et al. (2023) extend this framework to include a wider range of oil and clean energy assets. They note heterogeneous dependence structures between the clean energy and oil markets. Foglia et al. (2022) construct a tail-event driven network across clean energy and oil firms and find that the connection across the markets is time varying. Furthermore, they observe a strong dependence across firms within the same sector (i.e., clean energy or oil), while the cross-sector dependence between oil and clean energy firms is more limited. Although copula models or quantile analyses could capture the tail risk of the oil and stock market nexus to some extent, the existing literature only applies these approaches based on daily or weekly data (Xiao et al., 2018; Zhang and Liu, 2018; Reboredo and Ugolini, 2016; Sukcharoen et al., 2014). In this study, we measure higher-moment connectedness between oil and clean energy prices using intraday data. High frequency intraday data contain richer and more valuable information about the asset price behavior allowing investors to grasp investment opportunities more effectively.

More recently, the literature has moved toward analyzing the relationship between oil and clean energy stock markets using multivariate network models. This allows documenting the bi-variate relationships across the markets, while controlling for the spillovers from other sectors. Ahmad (2017) finds that technology and clean energy stocks are net emitters of returns, while crude oil is the net receiver. Ferrer et al. (2018) study the time-frequency connectedness between renewable energy stocks and crude oil prices and note similar results. Xia et al. (2019) examine the extreme connectedness between energy prices and renewable energy stocks and determine that clean energy stocks are net risk transmitters under extreme conditions. Saeed et al. (2021) analyze the extreme return connectedness between clean and dirty investments and find evidence of a stronger connectedness at the tails than at the mean of the return distributions. In this study, we extend the existing literature by conducting both static and dynamic analyses on the connectedness between clean energy stocks and oil prices at higher-order moments and examine the heterogenous roles of oil and clean energy markets in shocks transmission.

3. Data sources and empirical methodology

Our empirical methodology consists of three steps. In the first step, we construct high order moments (i.e., realized volatility, jump volatility, realized skewness, and realized kurtosis) using five-minute data on clean energy stock and oil prices. Using the realized high-moment measures, in the second step, we estimate the total, directional, and net connectedness among the markets using a time-varying parameter vector autoregression (TVP-VAR) model. In the third step, using regression analysis, we explore the roles of macroeconomic, financial, and environmental variables in determining the spillovers in higher-order moments among the clean energy and oil markets.

3.1. Realized variance, skewness and kurtosis

Following Andersen and Bollerslev (1998), Barndorff-Nielsen et al. (2010) and Baruník et al. (2015, 2017), we use realized variance as a measure of clean energy and oil market volatilities. Specifically, the realized variance (RV_t) is given by the following equation:

$$RV_t = \sum_{s=1}^{N} r_{s,t}^2, t = 1, 2, \ldots, T \tag{1}$$

where t denotes a trading day and s denotes a five-minute interval within the trading day. $r_{s,t}$ is the intraday return during interval s obtained by log-differencing the five-minute prices.

Next, we calculate the jump component of realized volatility. The realized volatility measure (RV_t) captures the average dispersion of financial returns during a given trading day. In contrast, the jump component of realized volatility captures any discontinuity in realized volatility. This has been shown to influence market spillovers significantly (Bonato et al., 2020; Gkillas et al., 2022; Hanif et al., 2023). In this paper, we first detect jumps using the threshold bi-power variation (TBPV) (Corsi et al., 2010). Specifically, the jump statistic $J_t^{(TBPV)}$ is calculated as follows:

$$J_t^{(TBPV)} = \sqrt{T}\,\frac{(RV_t - TBPV_t)RV_t^{-1}}{\left[(\zeta_1^{-4} + 2\zeta_1^{-2} - 5)max\left\{1, TQ_t TBPV_t^{-2}\right\}\right]^{1/2}} \tag{2}$$

where $\zeta_1 = \sqrt{2/\pi}$; $TQ_t = T\zeta_{4/3}^{-3}\sum_{s=1}^{N}\left|r_{t,s}\right|^{4/3}\left|r_{t,s+1}\right|^{4/3}\left|r_{t,s+2}\right|^{4/3}$ is the realized tri-power quarticity and converging in probability to integrated quarticity. The jump statistic $J_t^{(TBPV)}$ follows the standard Gaussian distribution. Next, using the results of the jump test, we calculate the jump component of volatility as follows:

$$J_t = \begin{cases} RV_t - TBPV_t \text{ if } J_t^{(TBPV)} > \Omega_\alpha \\ 0 \text{ otherwise} \end{cases} \tag{3}$$

where Ω_α denotes the critical value of a Gaussian distribution for an α significant level. $TBPV_t$ is the threshold bi-power variation, which is an estimate for the jump-free component of volatility and is given by: $TBPV_t = \sum_{s=2}^{N}\left|r_{t,s-1}\right|, \left|r_{t,s}\right|I_{\left\{\left|r_{t,s-1}\right|^2 \le \theta_{i-1}\right\}}I_{\left\{\left|r_{t,s-1}\right|^2 \le \theta_i\right\}}$, where $I_{\{\bullet\}}$ represents an indicator function, $r_{t,s}$ is the intraday return series, and Θ is the threshold function.

Finally, we calculate two additional higher-moment realized measures (i.e., skewness and kurtosis) to capture the asymmetry and tail risks in asset returns. The realized skewness (RS_t) can be expressed as:

$$RS_t = \frac{\sqrt{N}\sum_{i=1}^{N} r_{t,s}^3}{RV_t^{3/2}} \tag{4}$$

And the realized kurtosis is given by:

$$RK_t = \frac{N\sum_{i=1}^{N} r_{t,s}^4}{RV_t^2} \tag{5}$$

3.2. TVP-VAR connectedness among higher moments

We estimate an extended joint dynamic connectedness network based on the generalized forecast error decomposition of a time-varying vector autoregression (TVP-VAR) model following Balcilar et al. (2021). This approach extends the connectedness approach of Diebold and Yilmaz (2009, 2012, 2014) that summarizes the multivariate risk transmissions within large networks of variables using vector autoregression, impulse response functions, and generalized forecast error variance decompositions. While the original connectedness model was able to capture the spillovers across many variables, one of its drawbacks is that it relies on the selection of an arbitrary rolling window to analyze the change in the spillovers over time. Another drawback is that it decomposes each variable's forecast error variance conditioning on other variables' shocks one at a time. To address these issues, Antonakakis et al. (2020) propose using a time-varying parameter vector autoregression (TVP-VAR) model within the connectedness framework that is not sensitive to the length of the rolling window, less prone to outliers, and more appropriate for a shorter time series. Lastrapes and Wiesen (2021) develop joint connectedness metrics that decompose each variable's forecast error variance conditional upon all other variables' shocks jointly. Balcilar et al. (2021) combine the approaches by Antonakakis et al. (2020) and Lastrapes and Wiesen (2021) to develop an extended joint connectedness model.

In this paper, we follow the extended joint connectedness approach by Balcilar et al. (2021) to analyze the time-varying spillovers across the clean energy and oil markets for the following reasons. The TVP-VAR Extended Joint Connectedness Model allows us to capture the time-varying spillovers across the clean energy and oil markets without the specification of arbitrary rolling windows, while reducing the sensitivity of our results to outliers. Furthermore, the TVP-VAR model allows parameters to change over time. Therefore, it adjusts better to parameter changes. We believe the adjustments of the parameters in the TVP-VAR setting and the model's independence of arbitrary rolling windows is applicable to our analysis of higher-order moments across the clean energy and oil markets. This allows the model to adjust to the various positive and negative shocks in the energy markets during our sampling periods, such as the 2014–2016 oil glut, the COVID-19 financial crisis, and the Russia-Ukraine war, together with a general increase in public awareness and investor preferences for renewable energy. Finally, since the model decomposes each variable's forecast error variance conditional upon all other variables' shocks jointly, this allows us to calculate the GFEVD and connectedness indexes more accurately as argued by Balcilar et al. (2021).

The extended joint connectedness model starts with the estimation of the following TVP-VAR model:

$$y_t = B_t z_{t-1} + u_t; u_t \sim N(0, \Sigma_t) \tag{6}$$

$$vec(B_t) = vec(B_{t-1}) + v_t; vt \sim N(0, R_t) \tag{7}$$

where y_t is an $n \times 1$ vector of volatility, jumps, skewness, or kurtosis. z_{t-1} is a matrix of the lagged values of y_t with the optimal lag length determined by the Bayesian information criterion (BIC). B_t is a matrix of the time-varying coefficients that follows a random walk process. u_t and v_t denote the error terms, while Σ_t and R_t denote their corresponding variance-covariance matrices. Following Balcilar et al. (2021), the TVP-VAR model is estimated using a Kalman filter with forgetting factors.

Next, we use the Wold representation theorem to transform the TVP-VAR model into a time-varying parameter vector moving average (TVP-VMA) model: $z_t = \sum_{i=1}^{p} B_{it} z_{t-i} + u_t = \sum_{j=0}^{\infty} A_{jt} u_{t-j}$, where $A_0 = I_n$. The H-step forecast error is computed as:

$$\zeta_t(H) = y_{t+H} - E(y_{t+H}|y_t, y_{t-1}, \ldots) = \sum_{h=0}^{H-1} A_{h,t} u_{t+H-h} \tag{8}$$

The forecast error covariance matrix of $\zeta_t(H)$ is given by:

$$E(\zeta_t(H)\zeta_t^T(H)) = \sum_{h=0}^{H-1} A_{h,t} \Sigma_t A_{h,t}^T. \tag{9}$$

Next, the joint connectedness indexes are calculated using a row-sum normalization method based on the goodness-of-fit matrix (R^2). Specifically, $S_{i\leftarrow,t}^{jnt,from}$ indicates the impact of all other variables on variable i and is calculated as follows:

$$S_{i\leftarrow,t}^{jnt,from} = \frac{E\left[\zeta_{i,t}^2(H)\right] - E\left[\zeta_{i,t}(H) - E(\zeta_{i,t}(H)) \,|u_{\forall \neq i,t+1}, \ldots, u_{\forall \neq i,t+H}\right]^2}{E\left[\zeta_{i,t}^2(H)\right]} \tag{10}$$

$S_{i\leftarrow,t}^{jnt,from}$ is the proportion of the H-step forecast error variance of variable i that can be explained by jointly conditioning on the future shocks of all of the other variables. Under this approach, no normalization is needed.

To calculate the spillovers from variable i to all of the other variables in the network, Balcilar et al. (2021) introduce multiple scaling factors (λ), specifically:

$$\lambda_i = \frac{S_{i\leftarrow,t}^{jnt,from}}{S_{i\leftarrow,t}^{gen,from}} \tag{11}$$

$$\lambda = \frac{1}{n}\sum\nolimits_i^n \lambda_i \tag{12}$$

where $S_{i\leftarrow,t}^{gen,from}$ is the spillover from all of the other variables to variable i under the original Diebold and Yilmaz (2009, 2012, 2014) framework. Thus, the spillovers from variable i to all of the other variables $(S_{i\leftarrow,t}^{gen,to})$ is calculated using the following steps:

$$jSOT_{ij,t} = \lambda_i gSOT_{ij,t} \tag{13}$$

$$jSOT_{ii,t} = 1 - S_{i\leftarrow,t}^{jnt,from} \tag{14}$$

$$S_{i\rightarrow,t}^{gen,to} = \sum\nolimits_{j=1,i\neq j}^{n} jSOT_{ij,t} \tag{15}$$

where $gSOT_{ij,t}$ is the spillover from variable j to variable i under the original Diebold and Yilmaz (2009, 2012, 2014) model.

The joint total connectedness index is given by:

$$jSOI_t = \frac{1}{n}\sum_{i=1}^{n} S_{i\leftarrow,t}^{jnt,from} == \frac{1}{n}\sum_{i=1}^{n} S_{i\rightarrow,t}^{jnt,to} \tag{16}$$

The joint net connectedness is given by:

$$S_{i,t}^{jnt,net} = S_{i\rightarrow,t}^{jnt,to} - S_{i\leftarrow,t}^{jnt,from} \tag{17}$$

The pairwise directional connectedness between variables i and j is given by:

$$S_{ij,t}^{jnt,net} = gSOT_{ji,t} - gSOT_{ij,t} \tag{18}$$

Higher $jSOI_t$ implies a higher level of spillovers in the system. A positive $S_{i,t}^{jnt,net}$ indicates that variable i is a net shock transmitter in the network. A positive $S_{ij,t}^{jnt,net}$ implies that the amount of shocks transmitted from variable j to variable i is larger than that in the opposite direction.

3.3. Data sources, descriptive statistics and preliminary analyses

To investigate the spillovers across clean energy stock and oil prices at higher moments, we collect intraday data at the five-minute frequency. Specifically, we use the WTI crude oil spot price as a proxy for oil prices and the NASDAQ OMX Biofuel, Wind, Solar, Renewable Energy Generation, and Energy Efficiency Indexes as proxies for different sectors of the clean energy stock market. We focus on individual sectors

of the clean energy market instead of using an aggregate stock index for the entire clean energy stock market to capture the heterogeneous relationship between clean energy subsectors and oil prices (Pham, 2019). We collect intraday clean energy stock price data from Bloomberg and intraday oil price data from FirstRateData. Our data set spans from October 13, 2010-November 30, 2022. The beginning of the sampling period is based on the availability of the data.

In Table 1, we provide summary statistics of realized volatility, the jump component, realized skewness, and realized kurtosis calculated for stocks in five clean energy sectors and the oil prices. It is evident that oil prices experience the greatest daily realized volatility and jumps (0.00583 and 0.00047, respectively) followed by the biofuel sector in the clean energy market (0.00056, 0.00039, respectively). Other clean energy sectors have relatively small daily volatility and jumps ranging between 0.00015 and 0.00006, 0.00003 and 0.00001, respectively. On average, the biofuel, solar, and oil markets are negatively skewed, whereas the wind, renewable energy generation, and the energy efficiency markets are positively skewed. We find realized kurtosis ranges from 5.32 to 9.67, indicating the return distributions for stocks in all clean energy sectors and oil prices have fatter tails compared with normal distribution. The Jarque-Bera tests provide additional evidence to the presence of asymmetry and tail risks for clean energy stock and oil prices. In fact, the Jarque-Bera tests reject the normal distribution hypotheses for all of the high-order moments. The ADF tests and Ljung-Box tests, which test for the unit root and autocorrelation, further confirm the validity of our sample for further analysis.

To illustrate the time series trend of the high-order moments in our sample period, we present the plots of realized volatility, jumps, the realized skewness, and realized kurtosis in Fig. 1. Plots of realized volatility in Fig. 1.1 reveal that turbulent time periods are associated with sharp increase in the realized volatility for both the clean energy and oil markets. For example, daily realized volatility for the clean energy sectors and the oil market appears to be high during the 2011 European debt crisis, between 2015 and 2016 during the oil price crash caused by the reduction in oil production and low demand for oil in developing countries, and between 2020 and 2022 during the Covid-19 induced market crash and the Russia-Ukraine war. Consistent evidence is observed in the plots of jumps as shown in Fig. 1.2 in which the dramatic surges in 2020 and early 2022 are of particular interest. The big jumps coincide with the Russia-Saudi Arabia oil price war during the Covid-19 pandemic in 2020 and the beginning of Russia-Ukraine War in 2022. Fluctuations are also observed in realized skewness (Fig. 1.3) and kurtosis (Fig. 1.4) throughout our sample period. In particular, substantial variations in price asymmetry and tail risks are documented for all clean energy sectors and oil prices around 2013 and 2017, possibly attributable to the global oil supply interruptions and oversupplies in these periods. Taken together, we find highly consistent time series variations across the clean energy sectors and the oil market. Such preliminary evidence points to the existence of high correlations between the clean energy and oil markets at high-order moments.

4. Empirical results

4.1. Static higher-order moment connectedness between clean energy stock and oil prices

In this section, we examine the high-order moment connectedness between clean energy stock and oil prices. We present the static

Table 1
Summary statistics.

	Mean	Std.Dev.	Skewness	Kurtosis	Jarque-Bera	ADF	Q	Q2
Table 1.1. Realized volatility								
BIO	0.00056	0.01452	39.11 *	1538.51 *	298,934,587.0 *	−22.37 *	0.03204	0.03903
SOLAR	0.00015	0.0003	9.87 *	140.21 *	2,430,098.3 *	−9.44 *	16,419.1 *	7482.2 *
WIND	0.00004	0.0004	53.81 *	2940.46 *	1.093e+09 *	−20.88 *	3.894	0.009755
REG	0.00006	0.0009	38.41 *	1493.36 *	281,630,996.7 *	−21.84 *	0.3128	0.04146
ENEF	0.00006	0.0002	13.92 *	265.67 *	8,823,238.1 *	−10.22 *	11,871.1 *	3806.7 *
Oil	0.00583	0.1496	32.52 *	1104.28 *	153,904,333.6 *	−19.77 *	2110.8 *	1221.6 *
Table 1.2. Jump component of realized volatility								
BIO	0.00039	0.01452	39.14 *	1540.07 *	299,541,732.5 *	−22.45 *	0.04689	0.03896
SOLAR	0.00001	0.00004	21.85 *	632.20 *	50,305,744.9 *	−20.50 *	287.2 *	655.4 *
WIND	0.00001	0.00042	54.86 *	3017.84 *	1.151e+09 *	−22.31 *	0.1155	0.01006
REG	0.00003	0.00088	38.84 *	1516.15 *	290,304,820.0 *	−22.44 *	0.05834	0.04019
ENEF	0.00000	0.00002	23.79 *	839.87 *	88,852,125.8 *	−19.95 *	18.31	0.2605
Oil	0.00047	0.01175	31.74 *	1088.94 *	149,638,138.9 *	−16.43 *	1576.5 *	735.0 *
Table 1.3. Realized Skewness								
BIO	−0.05	0.93	−0.63 *	13.47 *	14,074.4 *	−22.02 *	23.83	55.3 *
SOLAR	−0.02	1.09	−0.13 *	7.15 *	2188.5 *	−22.54 *	28.31	71.9 *
WIND	0.01	1.54	0.09 *	4.38 *	244.8 *	−21.50 *	27.82	28.77
REG	0.02	1.04	0.29 *	9.52 *	5423.5 *	−21.85 *	36.4	48.9 *
ENEF	0.01	0.95	0.13 *	6.55 *	1598.4 *	−23.58 *	34.5	12.78
Oil	−0.01	1.15	−0.14 *	8.65 *	4043.8 *	−23.11 *	27.36	150.2 *
Table 1.4. Realized Kurtosis								
BIO	5.32	4.1	7.65 *	93.94 *	1,075,553.3 *	−6.43 *	76.2 *	45.1 *
SOLAR	6.07	4.11	6.22 *	73.03 *	639,654.9 *	−5.77 *	237.6 *	31.25
WIND	9.67	5.81	3.67 *	26.32 *	75,574.4 *	−4.83 *	88.3 *	39.9
REG	5.91	4.15	7.73 *	108.09 *	1,426,800.2 *	−5.61 *	117.1 *	6.035
ENEF	5.43	3.11	6.81 *	116.80 *	1,661,098.7 *	−4.98 *	85.4 *	5.186
Oil	6.06	4.74	6.53 *	75.28 *	682,177.4 *	−5.88 *	274.5 *	180.0 *

Notes: No. of observations: 3035. * indicates significance at the 5 % level. Jarque-Bera stands for the Jarque-Bera test for the null hypothesis of a normal distribution. ADF indicates the unit root test of Dickey and Fuller (1979) that checks the null hypothesis of the unit root for the residuals. Q and Q2 signify the Ljung-Box tests on the original series and its squared terms. BIO, SOLAR, WIND, REG, ENEF represent the NASDAQ OMX Biofuel, Wind, Solar, Renewable Energy Generation, Energy Efficiency Indexes. Oil signifies the oil market. The higher-order moments of all variables are estimated using intra-day five-minute return data where returns are calculated by log-differencing the intraday prices.

connectedness results in Table 2. In each sub-table, the numbers reported in the top six rows reflect the forecast error variance (in percentage terms) explained by the variables shown in the corresponding columns. Total connectedness received by each market from all other markets is reported in the last column "FROM," while total connectedness transmitted by each market to all other markets in the system is reported in the row "TO." The row "Inc. Own" presents the total spillovers from each market to all markets including itself. The row "NET" captures the net connectedness where positive (negative) values indicate a net shock transmitter (receiver). "TCI" denotes the total connectedness index reflecting the overall degree of connectedness in the system.

Considering the overall connectedness, TCI is 73.84 for realized volatility (Table 2.1), 73.30 for jumps (Table 2.2), 29.72 for skewness (Table 2.3), and 20.14 for kurtosis (Table 2.4). Our results indicate that clean energy sectors and the oil market are highly connected at all high-order moments. Furthermore, realized volatility and jump spillovers are the dominant determinants of the interdependence among the clean energy and oil markets. However, analyzing the spillovers in skewness and kurtosis still adds valuable information about the dynamics of the clean energy and oil markets since significant spillovers (more than 20 %) still exist at these higher-order moments.

Table 2 also reveals the major shock transmitters and receivers at each moment. For volatility spillover effects (Table 2.1), the oil market is the largest shock transmitter where the "TO" and "NET" connectedness indexes are 150.69 and 113.32, which is substantially higher than

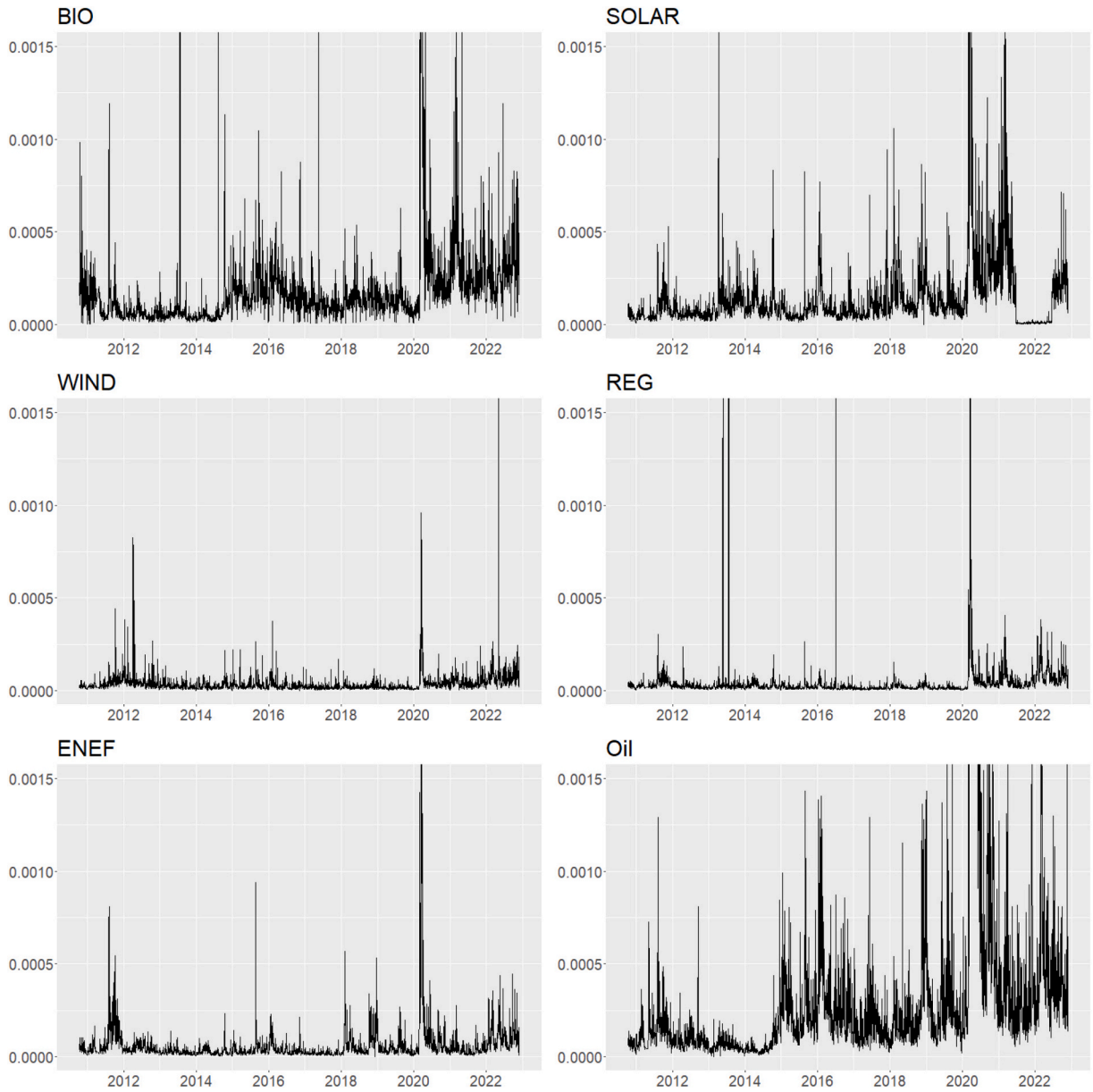

Fig. 1. Time series plots of realized volatility, jumps, realized skewness and realized kurtosis.
Fig. 1.1 Realized volatility.
Fig. 1.2 Jump component of realized volatility.
Fig. 1.3 Realized skewness.
Fig. 1.4 Realized Kurtosis.
Note: The figure plots the daily time series of the higher-order moments of clean and oil returns. BIO, SOLAR, WIND, REG, ENEF represent the NASDAQ OMX Biofuel, Wind, Solar, Renewable Energy Generation, Energy Efficiency Indexes. Oil signifies the oil market. The higher-order moments of all variables are estimated using intra-day five-minute return data where returns are calculated by log-differencing the intraday prices.

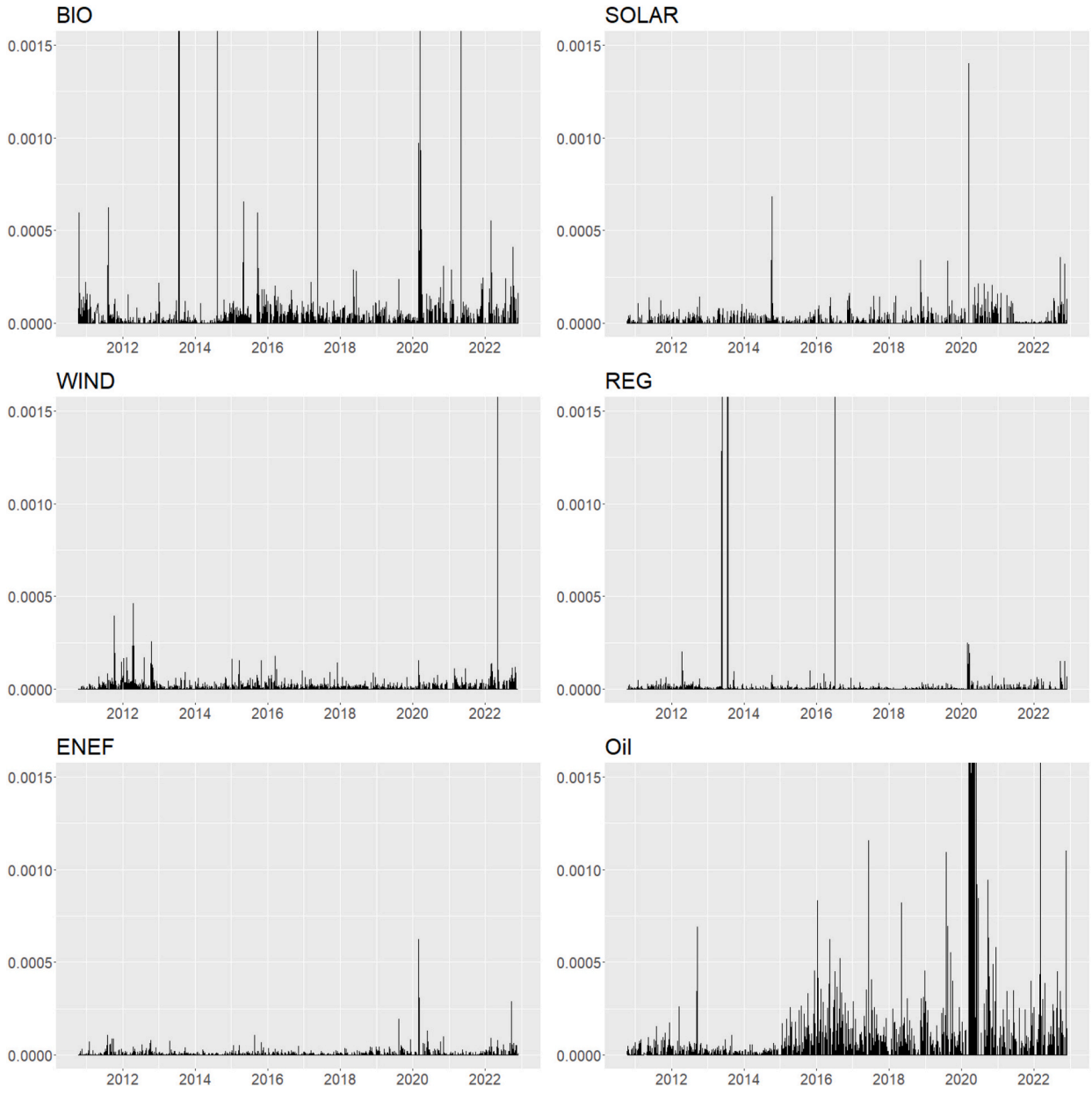

Fig. 1. (*continued*).

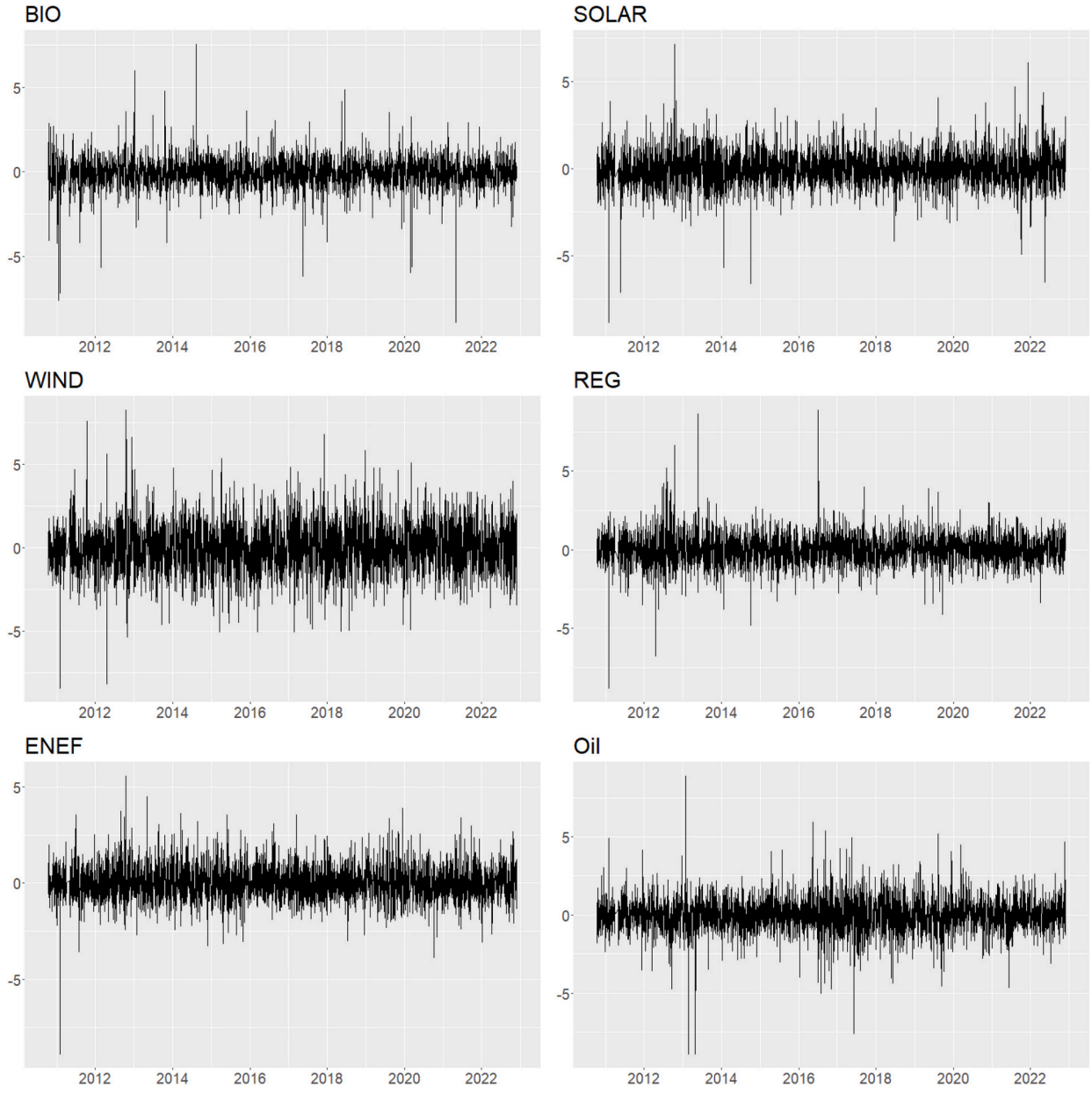

Fig. 1. (*continued*).

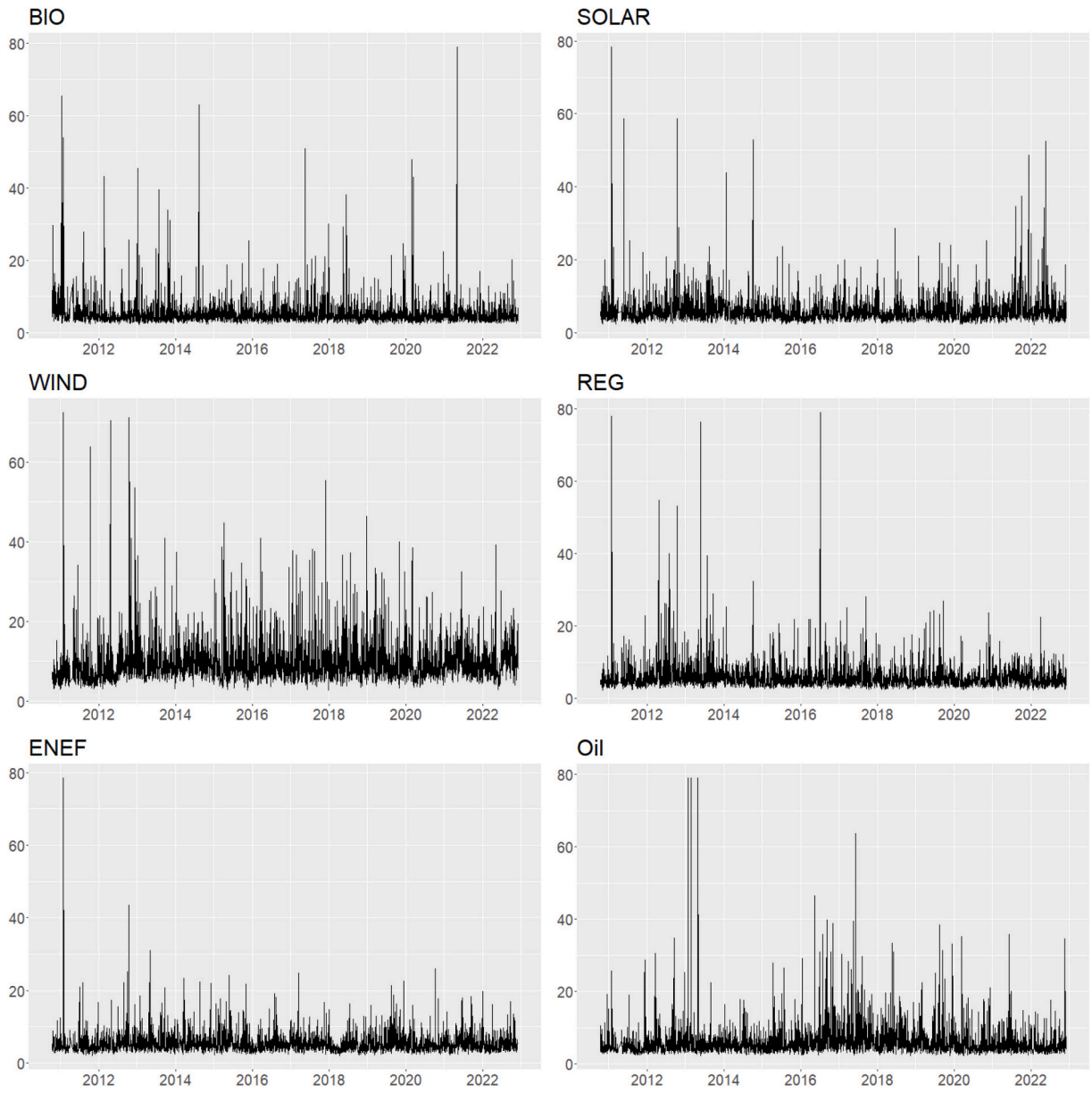

Fig. 1. (*continued*).

the other markets. All clean energy sectors are the net shock receivers with the biofuel sector being the largest receiver. For jump spillover effects (Table 2.2), the oil and biofuel markets are the largest shock transmitters in the system. The "TO" connectedness index is 101.97 for the oil market and 115.42 for the biofuel market, while the "NET" connectedness index is 28.31 for the oil market and 50.52 for the biofuel market. Solar, wind, and renewable energy generation sectors are net shock receivers with NET connectedness indexes ranging from −29.44 to −4.09. Note that the oil market plays a different and less significant role in determining the spillover effects in skewness and kurtosis (Tables 2.3 and 2.4). For example, oil becomes a net receiver of shocks in the third and fourth moments, while biofuel and the renewable energy generation sectors become the net shock transmitter. Our results expand the results of previous research that finds the shock receiver role of oil prices in the first moment in a system of oil, clean energy, and technology stock markets (Pham, 2019; Nasreen et al., 2020). We argue that the relationships between oil prices and clean energy stocks are moment dependent. Specifically, while oil shocks are important in determining the spillovers across the oil and clean energy markets in volatilities, clean energy markets drive the pattern of shock spillovers in tail events that are captured by the skewness and kurtosis spillover matrices.

Moreover, Table 2 suggests that the own-market spillover effects (shown diagonally in the tables) are stronger than the cross-market spillover effects. In other words, shocks within each market account for the largest share of forecast error variance. The own-market spillover effects also increase with the increase of moment orders (from Table 2.1 to Table 2.4) consistent with the findings of Zhang et al. (2023) and Foglia et al. (2022) that each market is primarily affected by its internal shocks.

Next, we discuss the spillover effects between the oil market and each clean energy sector. Table 2 suggests a significant role of the oil market in determining the behavior of the clean energy markets in realized volatility and its jump component. Specifically, in these two moments, the spillovers from the oil to the clean energy markets are typically more than 17 %, ranging from 17.43 to 37.39 %. Alternatively, the volatility and jump spillovers from the clean energy markets to the oil market are more limited. Clean energy markets typically account for less than 15 % of shocks in oil's realized volatility and jump component

Table 2
Average higher-order moment connectedness across clean energy stock and oil prices.

Table 2.1: Realized volatility

	BIO	SOLAR	WIND	REG	ENEF	Oil	FROM
BIO	23.89	7.72	9.65	21.48	9.18	28.08	76.11
SOLAR	7.07	11.42	12.97	11.37	25.27	31.91	88.58
WIND	6.41	13.3	14.38	10.51	18.01	37.39	85.62
REG	16.09	10.97	7.57	32.87	10.47	22.03	67.13
ENEF	8.36	22.77	14.57	11.24	11.78	31.28	88.22
Oil	2.91	4.94	15.2	4.08	10.23	62.64	37.36
TO	40.84	59.7	59.97	58.68	73.16	150.69	TCI
Inc.Own	64.72	71.12	74.35	91.55	84.94	213.32	73.84
NET	−35.28	−28.88	−25.65	−8.45	−15.06	113.32	

Table 2.2: Jump component of realized volatility

	BIO	SOLAR	WIND	REG	ENEF	Oil	FROM
BIO	35.09	9.03	9.98	16.62	7.33	21.94	64.91
SOLAR	19.37	22.83	12.78	12.53	12.53	19.97	77.17
WIND	25.52	11.5	20.17	11.46	10.2	21.14	79.83
REG	22.03	10.44	10.02	32.69	7.4	17.43	67.31
ENEF	18.42	14.09	12.33	10.58	23.09	21.5	76.91
Oil	30.08	10.77	10.76	12.03	10.01	26.34	73.66
TO	115.42	55.83	55.87	63.22	47.47	101.97	TCI
Inc.Own	150.52	78.66	76.04	95.91	70.56	128.31	73.30
NET	50.52	−21.34	−23.96	−4.09	−29.44	28.31	

Table 2.3: Realized skewness

	BIO	SOLAR	WIND	REG	ENEF	Oil	FROM
BIO	86.28	2.19	2.01	4.17	4.01	1.34	13.72
SOLAR	2.4	58.6	2.36	22.64	12.51	1.49	41.4
WIND	2.46	2.61	74.1	15.18	4.64	1.01	25.9
REG	4.23	20.84	12.08	45.57	16.1	1.18	54.43
ENEF	3.86	10.62	3.72	14.98	64.6	2.22	35.4
Oil	1.54	1.42	0.87	1.31	2.34	92.52	7.48
TO	14.48	37.7	21.04	58.28	39.6	7.24	TCI
Inc.Own	100.76	96.3	95.14	103.85	104.2	99.77	29.72
NET	0.76	−3.7	−4.86	3.85	4.2	−0.23	

Table 2.4: Realized kurtosis

	BIO	SOLAR	WIND	REG	ENEF	Oil	FROM
BIO	91.22	1.41	1.68	2.43	2.59	0.67	8.78
SOLAR	1.38	76.26	1.64	12.51	7.01	1.2	23.74
WIND	1.49	1.83	82.31	10.34	3.07	0.96	17.69
REG	2.26	12.21	8.84	62.41	12.66	1.63	37.59
ENEF	2.67	6.5	2.6	12.16	73.78	2.29	26.22
Oil	1.01	1.09	0.92	1.72	2.12	93.15	6.85
TO	8.81	23.04	15.68	39.15	27.44	6.75	TCI
Inc.Own	100.02	99.31	97.98	101.56	101.23	99.9	20.14
NET	0.02	−0.69	−2.02	1.56	1.23	−0.1	

Note: Each cell captures the spillovers from the column variable to the row variable. The column FROM captures the spillover from all of the other variables to the row variable. The row TO captures the spillover from the column variable to all of the other variables. The row Inc. Own captures the amount of spillover from the column variable to all of the variables including itself. The row NET captures the net spillover where positive (negative) values indicate net shock transmitters (receivers). The total connectedness index (TCI) is listed at the bottom right corner of the table. BIO, SOLAR, WIND, REG, ENEF represent the NASDAQ OMX Biofuel, Wind, Solar, Renewable Energy Generation, Energy Efficiency Indexes. Oil signifies the oil market. The higher-order moments of all variables are estimated using intra-day five-minute return data where returns are calculated by log-differencing the intraday prices.

with the exception of the biofuel market. Specifically, biofuel jumps account for 30.08 % of the forecast error variance in oil jumps. One explanation is that biofuel and oil are considered close substitutes. Thus, a jump in biofuel prices can lead to a significant jump in oil prices. Moreover, we find a smaller spillover effect between oil prices and clean energy prices at the third and fourth moments.

Finally, Table 2 also allows us to identify the connectedness pattern across the clean energy sectors. Our results suggest that although the total connectedness index declines as we move from lower to higher-order moments, significant pairwise spillovers still exist at the higher-order moments. For example, we find significant spillovers from the renewable energy generation sector to the solar, wind, and energy efficiency sectors (>10 %) in realized skewness and kurtosis. This highlights the relevance of analyzing the spillovers across the clean energy and oil markets at higher-order moments.

To better visualize the connectedness network between the clean energy sectors and the oil market, we present the connectedness graph in Fig. 2. As shown by the pairwise directional spillover measures, oil markets and clean energy sectors are highly connected in volatility and jumps, but less connected in skewness and kurtosis. Consistent with

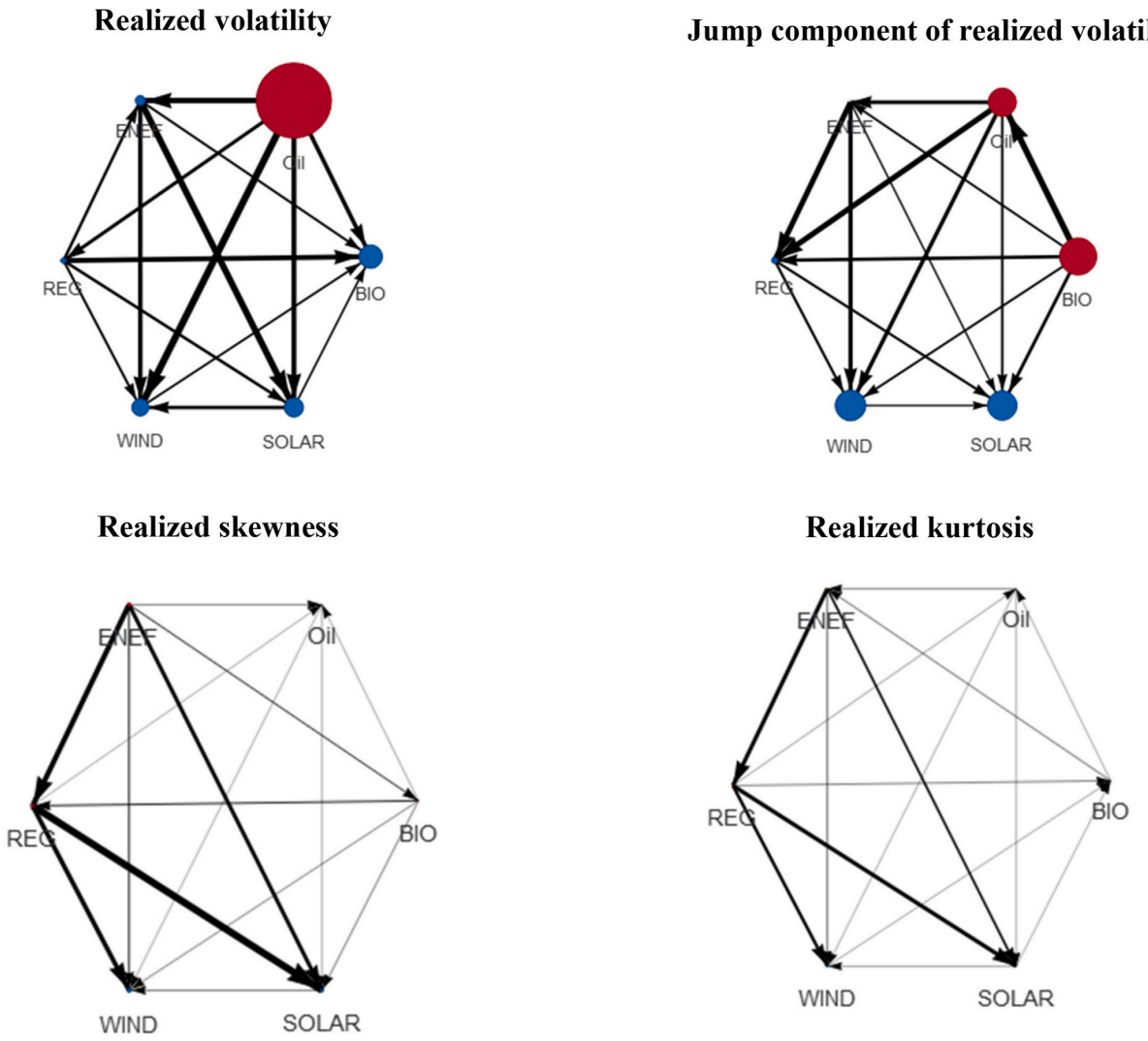

Fig. 2. Network connectedness.
Fig. 2.1 Realized volatility.
Fig. 2.2 Jump component of realized volatility.
Fig. 2.3 Realized skewness.
Fig. 2.4 Realized kurtosis.
Note: Red (blue) nodes indicate net shock transmitters (receivers). The size of the nodes indicates the magnitude of the net spillover indexes. The direction of the arrows captures the direction of spillovers between any two variables and the arrows' thickness capture the strength of the pairwise spillovers. BIO, SOLAR, WIND, REG, and ENEF represent the NASDAQ OMX Biofuel, Wind, Solar, Renewable Energy Generation, and Energy Efficiency Indexes. Oil signifies the oil market. The higher-order moments of all of the variables are estimated using intra-day five-minute return data where returns are calculated by log-differencing the intraday prices.

Table 2, the net shock transmitter and recipient roles played by these markets vary across moments and are more pronounced in volatility and jump spillovers, but weaker in skewness and kurtosis spillovers. Our findings indicate that when a low probability event occurs, connectedness between the oil and clean energy markets still persists. However, different markets may experience different reactions (Zhang et al., 2023).

4.2. Time-varying higher-order moments connectedness across oil and clean energy stocks

We next examine the time dynamics of connectedness by plotting the TCI and NET connectedness indexes over our sample period and present the plots in Figs. 3 and 4. In Figs. 3.1 and 3.2, the TCIs show generally consistent trends for volatility and jumps. Specifically, the total connectedness indexes for volatility and jump fluctuate between 2010 and 2017, drop to relatively low levels in 2018 and 2019, peak in 2020, and then remain at relatively high levels afterward. The peaks of connectedness in 2020 coincide with the Russia-Saudi Arabia oil price war during the Covid-19 pandemic. Together with other turbulent events, such as the Russia-Ukraine war, Figs. 3.1 and 3.2 indicate a high level of connectedness among the markets since 2020. In Figs. 3.3 and 3.4, the TCIs of skewness and kurtosis demonstrate similar trends throughout the sample period, but with relatively stronger variation documented for the kurtosis TCI. For both skewness and kurtosis, TCIs are comparatively high during the 2011 European debt crisis, the 2015 oil price crash, the 2020 Russia-Saudi Arabia oil price war during the Covid-19 pandemic, and the 2022 Russia-Ukraine war. Overall, our results indicate that total connectedness indexes at high-order moments are time varying and tend to strengthen with instable oil markets and worsening economic conditions. The finding of intensified connectedness during turbulent periods is consistent with previous studies

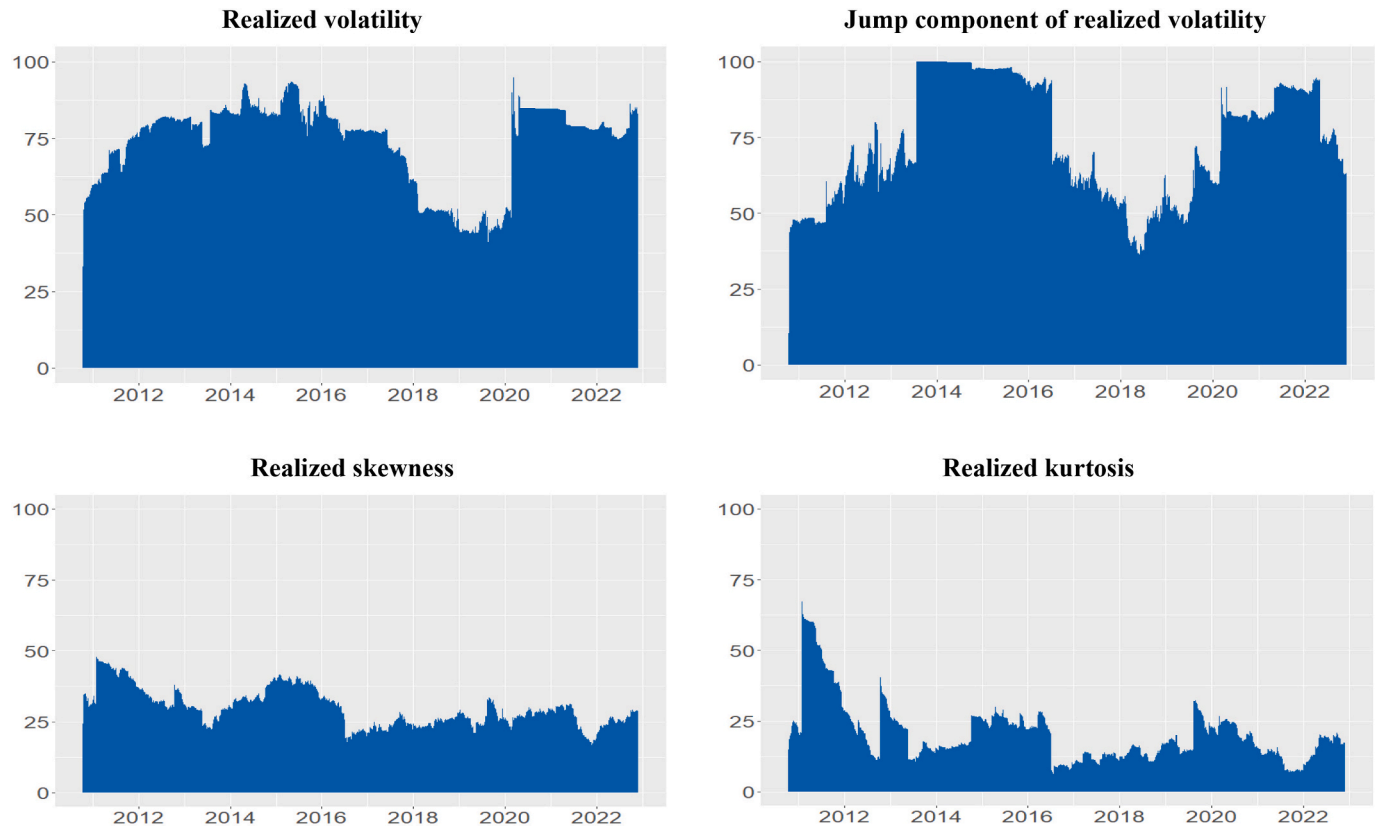

Fig. 3. Total connectedness indexes.
Fig. 3.1 Realized volatility.
Fig. 3.2 Jump component of realized volatility.
Fig. 3.3 Realized skewness.
Fig. 3.4 Realized kurtosis.
Note: The figure presents the total connectedness indexes among clean energy and oil markets in higher-moments using the TVP-VAR Joint Connectedness approach.

including Reboredo (2015), Reboredo and Ugolini (2016), Naeem et al. (2020) and Zhang et al. (2023). As suggested by Bakas and Triantafyllou (2018) and Bouri et al. (2021), macroeconomic uncertainties can translate into rising uncertainty about future aggregate demand and supply. Given that commodity prices are highly sensitive to aggregate demand and supply conditions, increases in the uncertainty surrounding the macroeconomy can lead to higher volatility in commodity prices. This effect spills over to other energy commodities and their volatilities. Our results complement these previous findings by providing additional evidence regarding the stronger spillover effects among higher-order moments during higher uncertainty periods.

We conduct similar time-series analyses using net connectedness indexes and present the plots in Fig. 4. Different from the total connectedness index in Fig. 3, the net directional measure of connectedness provides useful information about the time varying role played by each market as net shock transmitter or receiver over our sample period. Specifically, a positive (negative) value in Fig. 4 indicates a net transmitter (receiver) role in connectedness of the corresponding market to (from) all of the other markets. Overall, we find that all net connectedness indexes display substantial variations over time with the largest net connectedness documented during the periods with unstable market conditions consistent with the findings in Fig. 3. In Fig. 4.1, the oil market is the main net shock transmitter of volatility connectedness most of the time, while the five clean energy sectors are primarily net shock recipients. In the 2020 Russia-Saudi Arabia oil price war and Covid-19 pandemic period, biofuel and renewable energy generation sectors experience a sharp increase in their net connectedness indexes and become net shock transmitters for a short period of time. This reflects an increase in public interest toward alternative energy in response to highly volatile oil prices during this period. In Fig. 4.2, the most noticeable changes of jump connectedness are identified in the biofuel sector, the energy efficiency sector, and the oil market. The strong positive net connectedness indexes suggest that these markets act as the biggest net shock transmitters most of the time. Solar and wind sectors remain the primary net shock receivers during the sample period, whereas the renewable energy generation sector shows small switches between these two roles. For the net connectedness in skewness as shown in Fig. 4.3, renewable energy generation and energy efficiency sectors become the major net shock transmitters, while solar and wind are the major net shock receivers. Biofuel and oil markets exhibit cycle changes between positive and negative values in net skewness connectedness. In Fig. 4.4, small constant fluctuations in net kurtosis connectedness are found for all markets indicating weak predictability of net kurtosis connectedness among these markets when low probability events occur. For all high-order moments, the time varying net connectedness of the clean energy and oil markets, together with their time varying net shock transmitter/receiver roles, are generally consistent with the previous findings documented in Table 2 and Figs. 2 and 3.

In summary, our connectedness results demonstrate large variations in the spillovers across clean energy and the oil markets at different moments. Oil is the dominant shock transmitter in volatility and jumps. However, its role fluctuates in skewness and kurtosis. Most clean energy markets are net shock receivers in volatility throughout our sampling period. However, they are more likely to switch to the net shock transmitter roles at higher moments (i.e., skewness and kurtosis). This reflects investors' interests in alternative energy under low probability events. Furthermore, we find that the fluctuations of the markets between the shock transmitter and receiver roles decrease at higher

moments. This indicates that the spillovers across the clean energy and oil markets are less predictable when low probability events occur. Finally, our results suggest the significant role of the second moments (i.e., volatility and its jump component) in explaining the overall interdependence among the clean energy and oil markets. However, an analysis of the spillovers at the third and fourth moments is still valuable as significant spillovers still exist among the markets at these moments. Our results also highlight the unpredictability of spillovers at higher-order moments, and empirical analyses that focus on the first and second moments may not be able to capture this unpredictability.

4.3. Does day-of-the-week effect exist for higher-order moments connectedness across oil and clean energy stocks?

In the earlier sections, we have studied the time dynamics of high-order moment connectedness over the entire sample period. To investigate the time varying behavior of connectedness further, we study TCI between the clean energy and oil markets across weekdays. To allow meaningful comparison, we match five non-missing weekdays from each same week and then calculate mean TCI on each weekday. This matching strategy enables us to compare connectedness variations across weekdays to identify day-of-the-week patterns holding the economic conditions during the week constant. We test the statistical significance of daily differences in TCI between two weekdays using a paired sample *t*-test.

As shown in Fig. 5, Panel A, the connectedness patterns in realized volatility, skewness, and kurtosis between clean energy stock and oil prices demonstrate similar overall trends from Mondays to Fridays. Specifically, the total connectedness index (TCI) appears to be the lowest on Mondays and gradually trends upward across the rest of the weekdays. For connectedness in volatility jump, there are changing dynamics from Tuesdays to Fridays. The TCI for volatility jump starts rising from the trading opening on Mondays and peaks on Tuesdays, but drops on Wednesdays and these changes are statistically significant at 1 % and 5

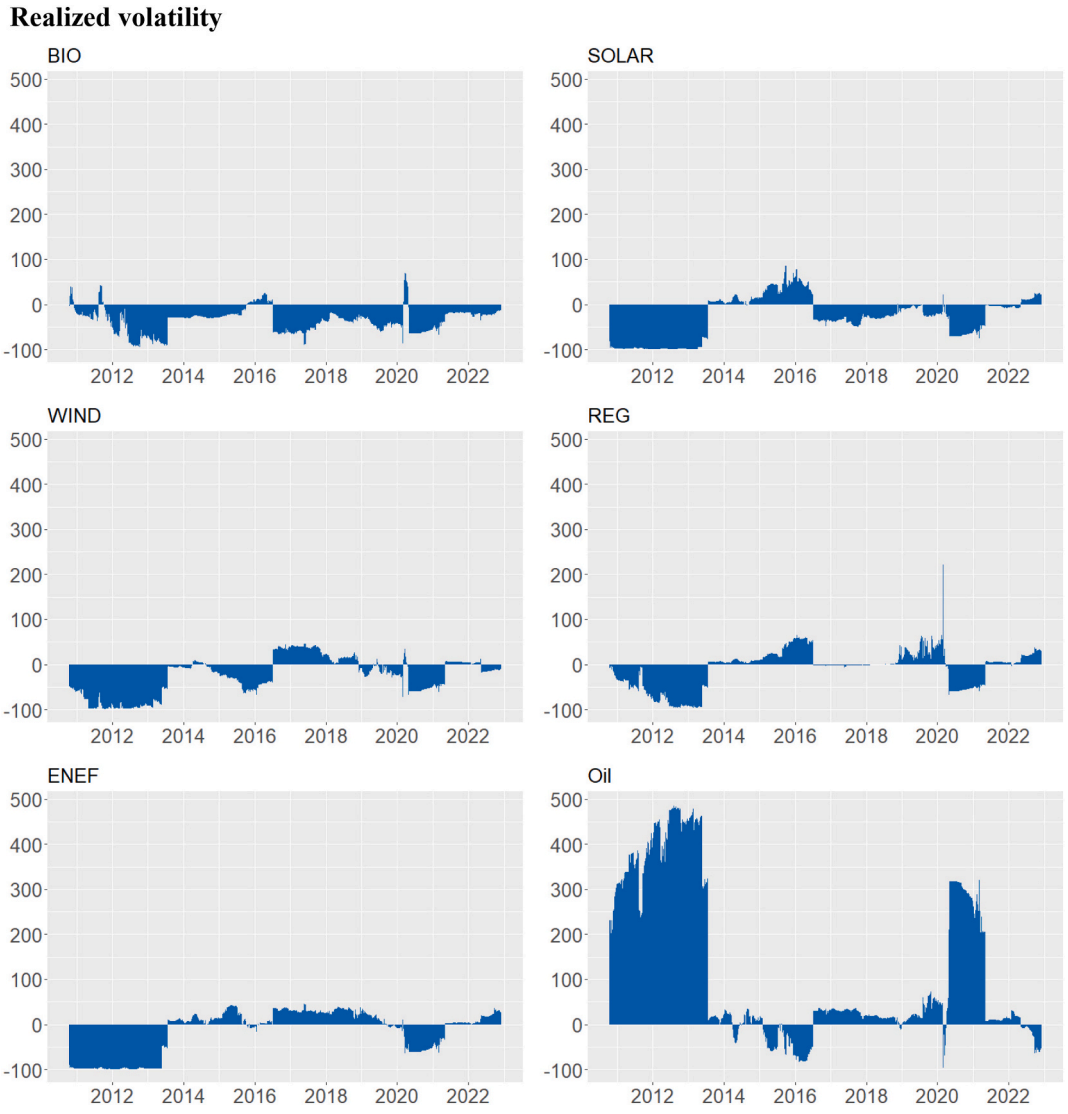

Fig. 4. Net connectedness indexes.
Fig. 4.1 Realized volatility.
Fig. 4.2 Jump component of realized volatility.
Fig. 4.3 Realized skewness.
Fig. 4.4 Realized kurtosis.
Note: The figure presents the time-varying net connectedness of clean energy and oil markets in higher moments. Positive (negative) values indicate a market is a net shock transmitter (receiver). BIO, SOLAR, WIND, REG, and ENEF stand for the NASDAQ OMX Biofuel, Wind, Solar, Renewable Energy Generation, and Energy Efficiency Indexes. Oil signifies the oil market.

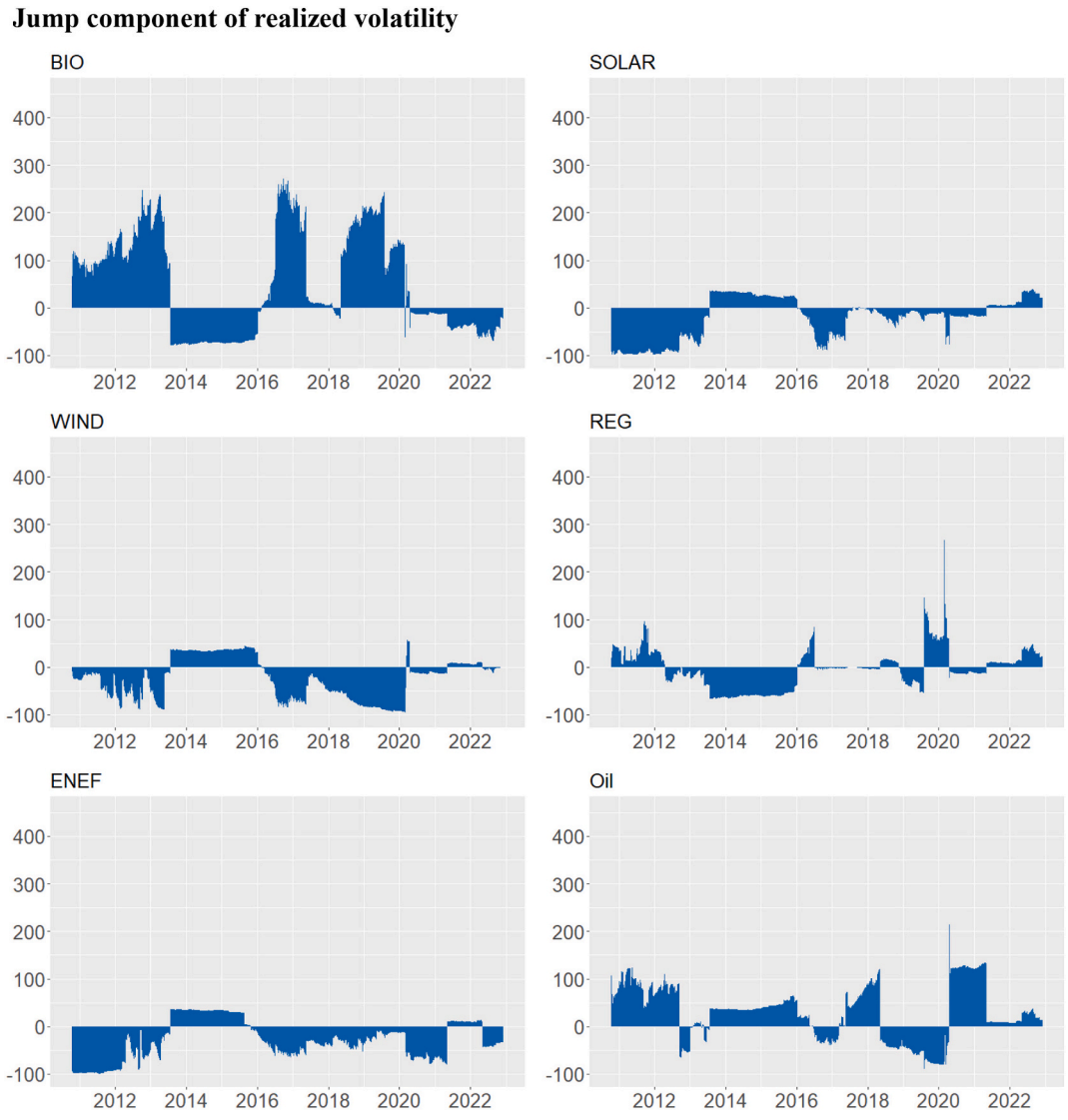

Fig. 4. (*continued*).

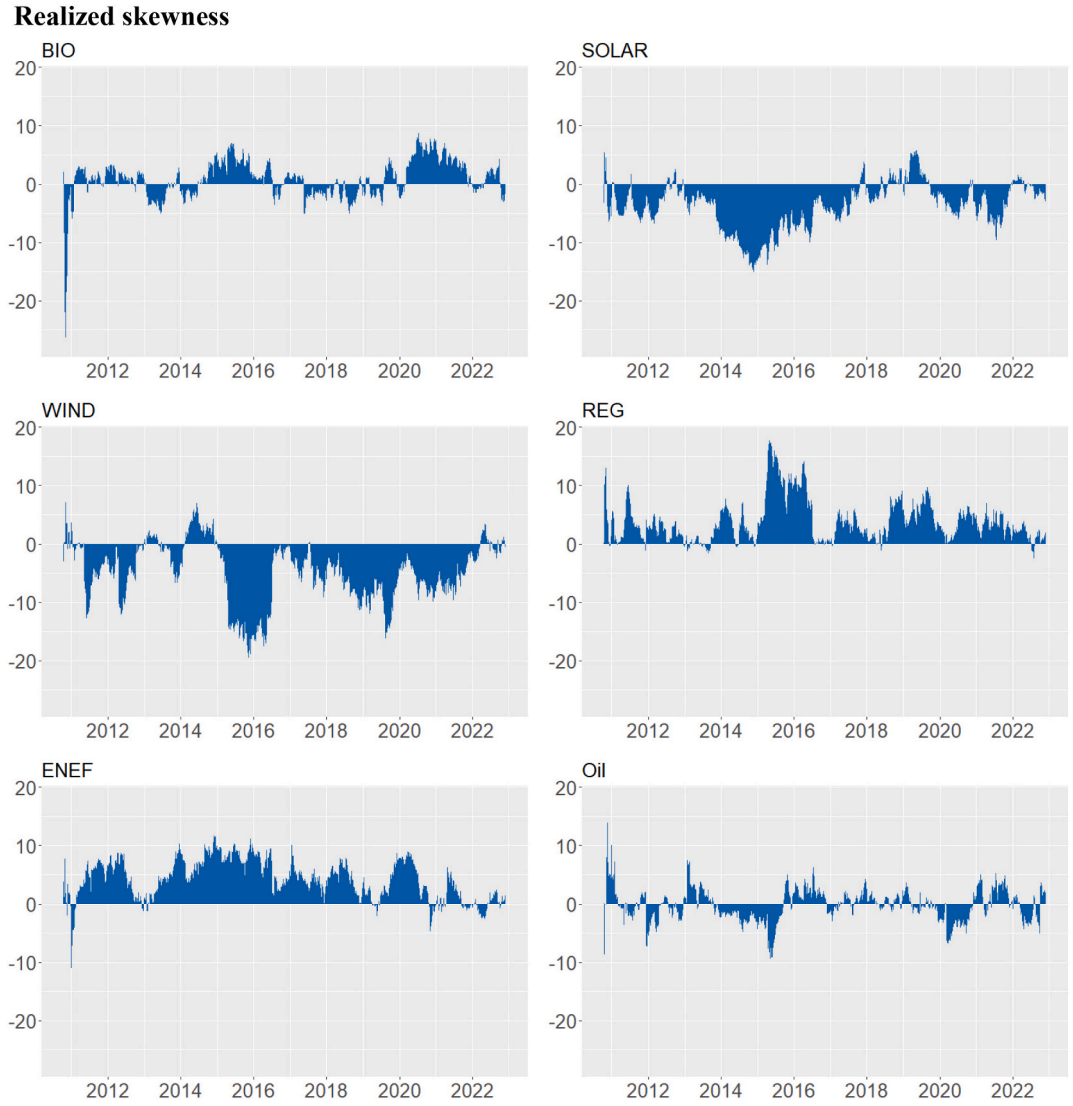

Fig. 4. (*continued*).

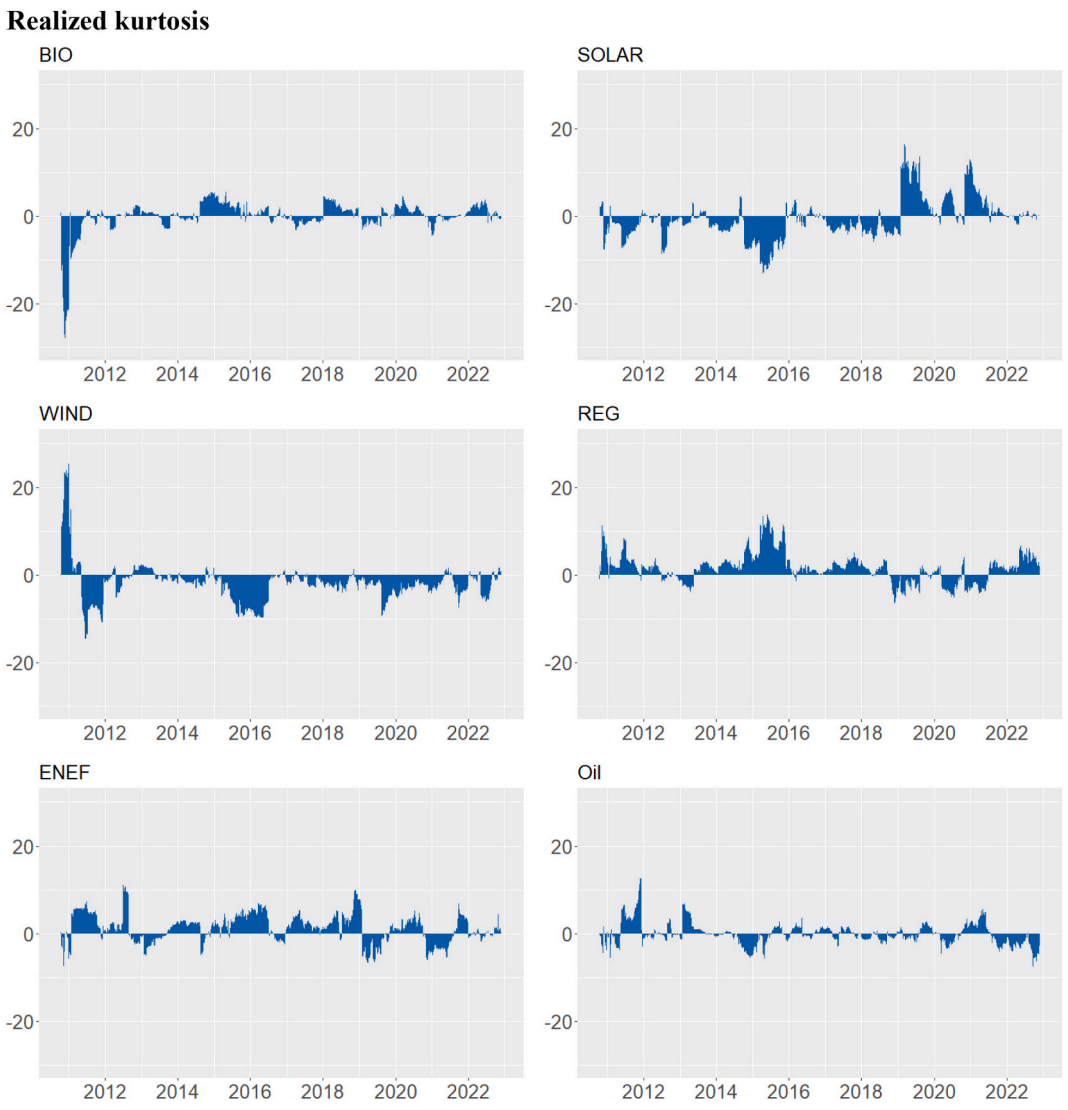

Fig. 4. (*continued*).

%, respectively. The degree of connectedness intensifies again on Thursdays and remains toward the closing of trading on Fridays. Since the jump component of volatility better captures the discontinuity in realized volatility, the fluctuations in the connectedness pattern reflect the changes in the market reactions due to the influx of news information around the middle of the week.

Overall, our results are complementary to the well documented Monday effect existing among stock returns in which stock returns have been found to be significantly lower on Mondays compared with other days within the week (Cross, 1973; French, 1980). Our findings corroborate that variation exists in the timing of releasing news information across weekdays. In particular, the number of public news announcements has been found to be low on Mondays, but increases from Tuesdays to Thursdays and then tapers off on Fridays (Mitchell and Mulherin, 1994). The relatively low connectedness between the clean energy stock market and the oil market on Mondays can be attributed to the initial lack of news information in the markets at the opening of the trading week. However, TCI strengthens as more news information is being released, incorporated, and accumulated throughout the rest of the trading week.

To explore the day-of-the-week connectedness patterns further, we partition our full sample periods into high uncertainty vs. low uncertainty periods based on the median values of the daily uncertainty indexes including the daily CBOE Oil Volatility Index (OVX), the VIX Volatility Index (VIX), Economic Policy Uncertainty (EPU), and the Geopolitical Risk Index (GPR). Specifically, if the value of the daily OVX/VIX/ EPU/GPR index is above its median value, the day is classified as high OVX/VIX/ EPU/GPR. Otherwise, the day is classified as low OVX/VIX/ EPU/GPR. Then, within each subsample, we match the five non-missing weekdays from each same week and calculate the mean TCI on each weekday for comparison. We present the plots in Figs. 5.2–5.5.

As shown in Fig. 5.2, during high OVX periods, TCI for realized volatility has an upward trend and TCI for volatility jumps exhibits more variable patterns across the five weekdays. These patterns are consistent with the overall connectedness patterns reported in Fig. 5.1. However, the connectedness at higher moments (i.e., skewness and kurtosis) weakens considerably from Wednesdays during high OVX periods. Intriguingly, the connectedness patterns for all high-order moments (except jumps) appear to be reversed in low OVX periods compared with high OVX periods indicating the time dynamics of TCI is highly dependent upon market uncertainty.

As illustrated in Figs. 5.3–5.5, the day-of-the-week connectedness patterns during high VIX/EPU/GPR periods persist consistently in general. With the exception of the connectedness of jumps during a high GPR period, total connectedness indexes are all trending upward across the five weekdays, consistent with the overall connectedness patterns

TCI

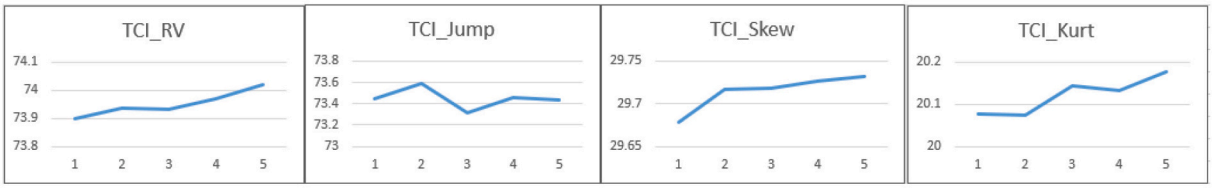

TCI in high OVX vs low OVX periods

High OVX

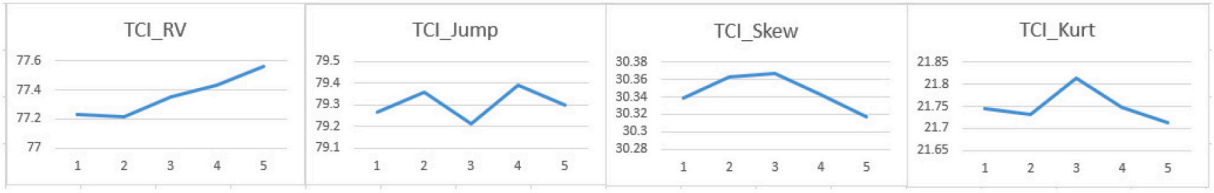

Low OXV

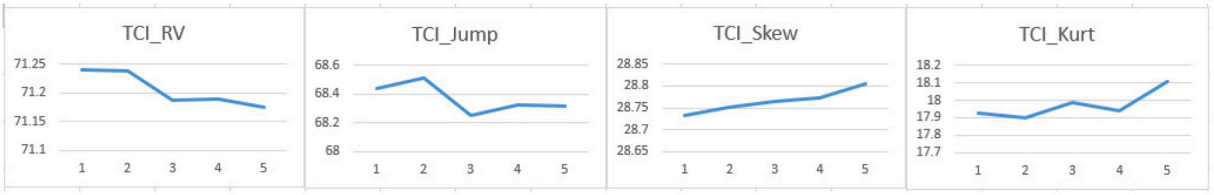

TCI in high VIX vs low VIX periods

High VIX

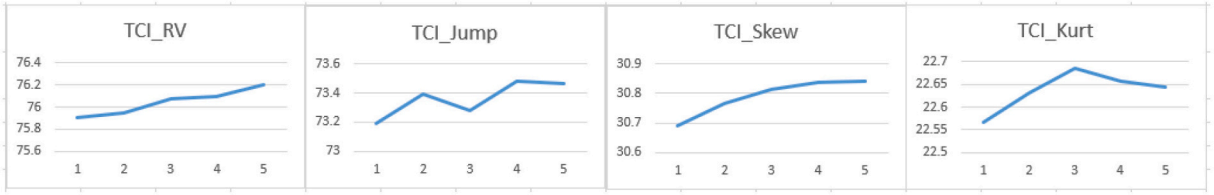

Low VIX

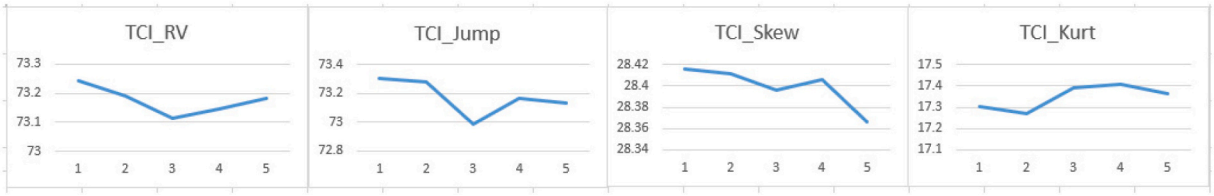

Fig. 5. Day-of-the-week patterns in connectedness between oil prices and green stocks. (For interpretation of the references to colour in this figure legend, the reader is referred to the web version of this article.)
Fig. 5.1 TCI.
Fig. 5.2 TCI in high OVX vs low OVX periods.
Fig. 5.3 TCI in high VIX vs low VIX periods.
Fig. 5.4 TCI in high EPU vs low EPU periods.
Fig. 5.5 TCI in high GPR vs low GPR periods.

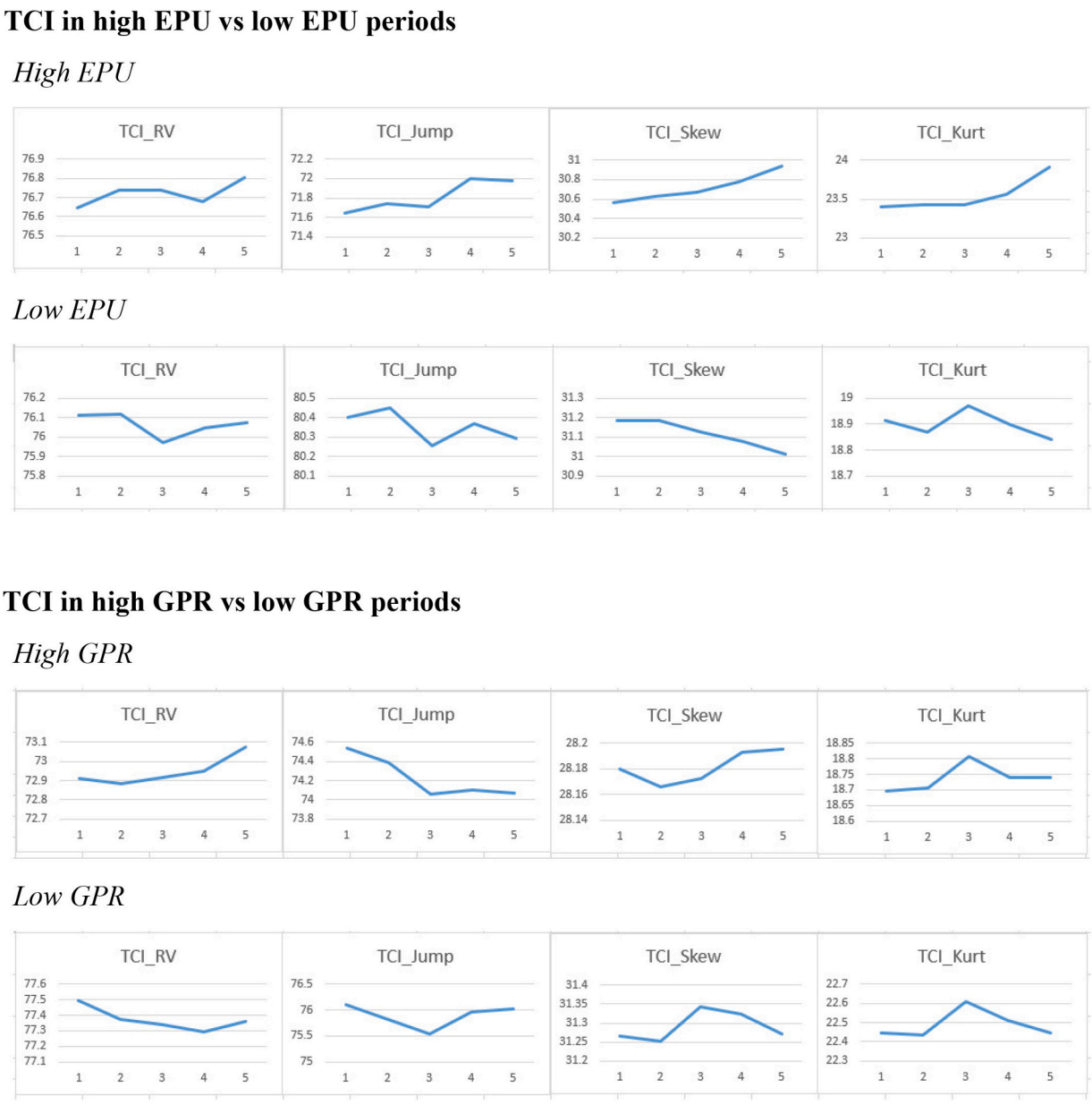

Fig. 5. (*continued*).

presented in Fig. 5.1. These results can be explained by the fact that the accumulation of news information is faster and steadier during a high uncertainty trading week, which increases the total connectedness indexes throughout the weekdays. In most cases, the connectedness for all high-order moments demonstrates opposite patterns during low VIX/EPU/GPR periods compared with high VIX/EPU/GPR periods. During low VIX/EPU/GPR periods, total connectedness indexes for all high-order moments are generally trending downward across the five weekdays.

Viewed collectively, the opposite patterns documented during low vs. high uncertainty periods have interesting implications. We find that connectedness tends to trend upward throughout the trading days within a week during turbulent periods with high uncertainty. This pattern is reversed during low uncertainty periods. It has been well established in the literature that the stock market tends to overreact to good news and underreact to bad news. When responding to negative information, investors initially demonstrate underreaction causing information to be incorporated into stock prices slowly and price continuation (or return drift) after the news shocks (Hong et al., 2000; Frank and Sanati, 2018). Our findings suggest that this momentum effect also exists in the higher moment connectedness. During turbulent periods with high uncertainty, investors underreact to the negative news released in the markets causing information to be incorporated into the prices of energy commodities slowly and gradually. The information is accumulated and spilled over across the energy markets throughout the trading days within a week leading to the upward day-of-the-week connectedness patterns at the higher-order moments. The reversed day-of-the-week connectedness patterns hold true when investors overreact to positive information during the low uncertainty periods.

4.4. Uncertainty and higher-order moment connectedness

Thus far, we have established the high-order moment connectedness between the clean energy and oil markets and have also studied the time dynamics of their connectedness. In addition, our analysis in Section 4.3 implies that the relationship between uncertainty factors and higher-order moment connectedness among oil and clean energy stocks is state-dependent. In this section, we further identify how the

Table 3
Uncertainty and the higher-moment connectedness between oil and clean energy stocks.

	(1)	(2)	(3)	(4)	(5)	(6)	(7)	(8)
Variable: TCI	RV	RV	Jump	Jump	Skewness	Skewness	Kurtosis	Kurtosis
State	Low connectedness	High connectedness	Low connectedness	High connectedness	Low connectedness	High connectedness	Low connectedness	High connectedness
OVX	−10.6130***	−3.8000***	10.6105***	−5.4398***	−2.5723***	−0.9197***	−5.1498***	2.6595***
	[1.2807]	[0.3646]	[1.6381]	[0.3780]	[0.2499]	[0.3150]	[0.2945]	[0.6530]
VIX	8.4199***	4.0047***	−7.4474***	−7.1421***	4.3765***	9.7466***	4.7509***	6.3735***
	[1.3514]	[0.5247]	[0.7685]	[0.7194]	[0.3090]	[0.5355]	[0.3122]	[0.8281]
EPU	3.1715***	1.1541***	1.1966**	−1.9603***	0.9774***	0.9148***	1.3244***	−0.8608*
	[0.6880]	[0.2070]	[0.4770]	[0.2093]	[0.1256]	[0.1648]	[0.1772]	[0.4807]
GPR	0.4954	−1.5230***	−2.3129***	0.0867	−0.6587***	0.2816	−0.0336	1.0830*
	[0.5177]	[0.2193]	[0.6115]	[0.2431]	[0.1678]	[0.3096]	[0.1879]	[0.6545]
Constant	48.8595***	82.9451***	46.8327***	139.9058***	19.9081***	3.7467*	11.8620***	2.2690
	[5.1641]	[1.7582]	[5.4109]	[1.5307]	[1.2150]	[1.9550]	[1.5314]	[4.0276]
ln(sigma)	1.8432***	1.4487***	2.1826***	1.2632***	0.8887***	1.3606***	0.9819***	2.2169***
	[0.0354]	[0.0196]	[0.0169]	[0.0199]	[0.0223]	[0.0290]	[0.0213]	[0.0291]
N	3056	3056	3056	3056	3056	3056	3056	3056

Note: Robust SE in brackets. *** $p < 0.01$, ** $p < 0.05$, * $p < 0.1$. OVX, VIX, EPU, GPR stands for the CBOE oil volatility index, CBOE VIX index, Economic Policy Uncertainty index, and geopolitical risk index. All regressions include dummies for the 2014–2016 oil glut, the COVID-19 financial crisis, and the Ukraine-Russia war period.

connectedness among oil and clean energy stocks is related to economic, political, and financial market uncertainty across high and low uncertainty states. To this end, we estimate the following Markov switching regression model[3]:

$$jSOI_t = \mu_{s,t} + \alpha_{s,t} UNC_t + \beta X_t + \epsilon_{s,t}; \epsilon_{s,t} \sim iid\left(0, \sigma^2_{s,t}\right) \tag{19}$$

where $jSOI_t$ denotes the total joint spillover index for volatility, the jump component of volatility, skewness, and kurtosis. UNC_t is a vector of uncertainty indexes that includes the CBOE oil volatility index (OVX), the CBOE VIX index (VIX), the Economic Policy Uncertainty index (EPU), and the geopolitical risk index (GPR). s denotes the state ($s_t \in [1, 2]$), and the effects of uncertainty factors can be switched between the states with the mean $\mu_{s,t}$ and variance, $\sigma^2_{s,t}$. X_t is a set of dummy variables to indicate the 2014–2015 oil glut, the COVID-19 financial crisis, and the Russia-Ukraine war. $\epsilon_{s,t}$ denotes the error term.

Table 3 presents the estimation results. The odd numbered columns indicate the effect of uncertainty variables on the connectedness across clean energy and oil prices during low connectedness periods, while the even numbered columns indicate the results for high connectedness periods. We find that oil price volatility (proxied by the OVX index) is associated with a decrease in connectedness among oil and clean energy stocks in most cases. This suggests that clean energy stocks tend to decouple from oil prices in response to increasing oil volatility. However, our results also show several exceptions to this decoupling pattern. For example, jump connectedness and kurtosis connectedness increase in response to increasing oil volatility during the low and high connectedness states, respectively. In addition, an increase in the VIX index (a proxy for stock market volatility) is associated with an increase in the connectedness across all the higher-order moments except for the jump component of volatilities. Moreover, an increase in the economic uncertainty index is associated with an increase in connectedness except for the jump and kurtosis connectedness during the high connectedness states. Note that the magnitude of the coefficients on economic policy uncertainty is smaller (in absolute value) than those on oil and stock market volatility. Finally, the effect of geopolitical risk on higher-order moment connectedness across clean energy and the stock markets is less statistically significant. Altogether, our results suggest that market volatility, such as oil and stock market volatility, are the main drivers of higher-order moment connectedness among clean energy stock and oil prices. Changes in the market volatility have a strong and direct impact on the higher-order moment connectedness between the oil and clean energy markets. In contrast, economic policy uncertainty and geopolitical risk play a more modest role. Despite the fact that economic uncertainty has been found to have strong impact on a single financial market (Gu et al., 2021; Zhang and Yan, 2020), our results suggest that it has a relatively weaker and indirect impact on cross-market connectedness. Economic uncertainty can be transmitted to the oil and clean energy markets by affecting the market volatility and financial investors' sentiment (Lyu et al., 2021; Bakas and Triantafyllou, 2018; Wang et al., 2023), both of which are captured in the measures of market volatility such as OVX and VIX, resulting in a strengthened impact of financial market volatility on oil and clean energy connectedness.[4]

5. Economic and financial implications

5.1. Utility-based hedge ratios

In previous sections, we demonstrate that there is a significant amount of spillovers among the clean energy and oil markets at higher-order moments. This highlights the relevance of considering these higher-order moments in designing investment strategies. In this section, we discuss the usefulness of incorporating higher-order moments in portfolio allocation decisions in terms of hedging effectiveness, utility, and the information ratio. Following Alexander and Barbosa (2008), we analyze how a long position in oil prices can be hedged by a short position in clean energy stocks. Let $r_{j,t}$ be the realized return for asset j ($j = Oil, Clean$) on day t. The return on a hedged portfolio (p) is given by:

$$r_{p,t} = r_{Oil,t} - \beta_t r_{Clean,t} \tag{20}$$

where β_t is the optimal hedge ratio for day t, which is chosen to maximize expected utility. The values of β_t depend on the functional form of

[3] The Markov Switching model assumes that the time series can switch between different regimes. TVP-VAR model extends the standard VAR framework by allowing the parameters to change over time. Both models intend to capture the dynamic changes in time series data. In this paper, we conduct a state-dependent connectedness analysis. In such a framework, the connectedness measures among oil and clean energy stocks can vary across different states, which provides insights as to how connections among variables change during different economic conditions.

[4] VIX is also well-known as a fear gauge indicator.

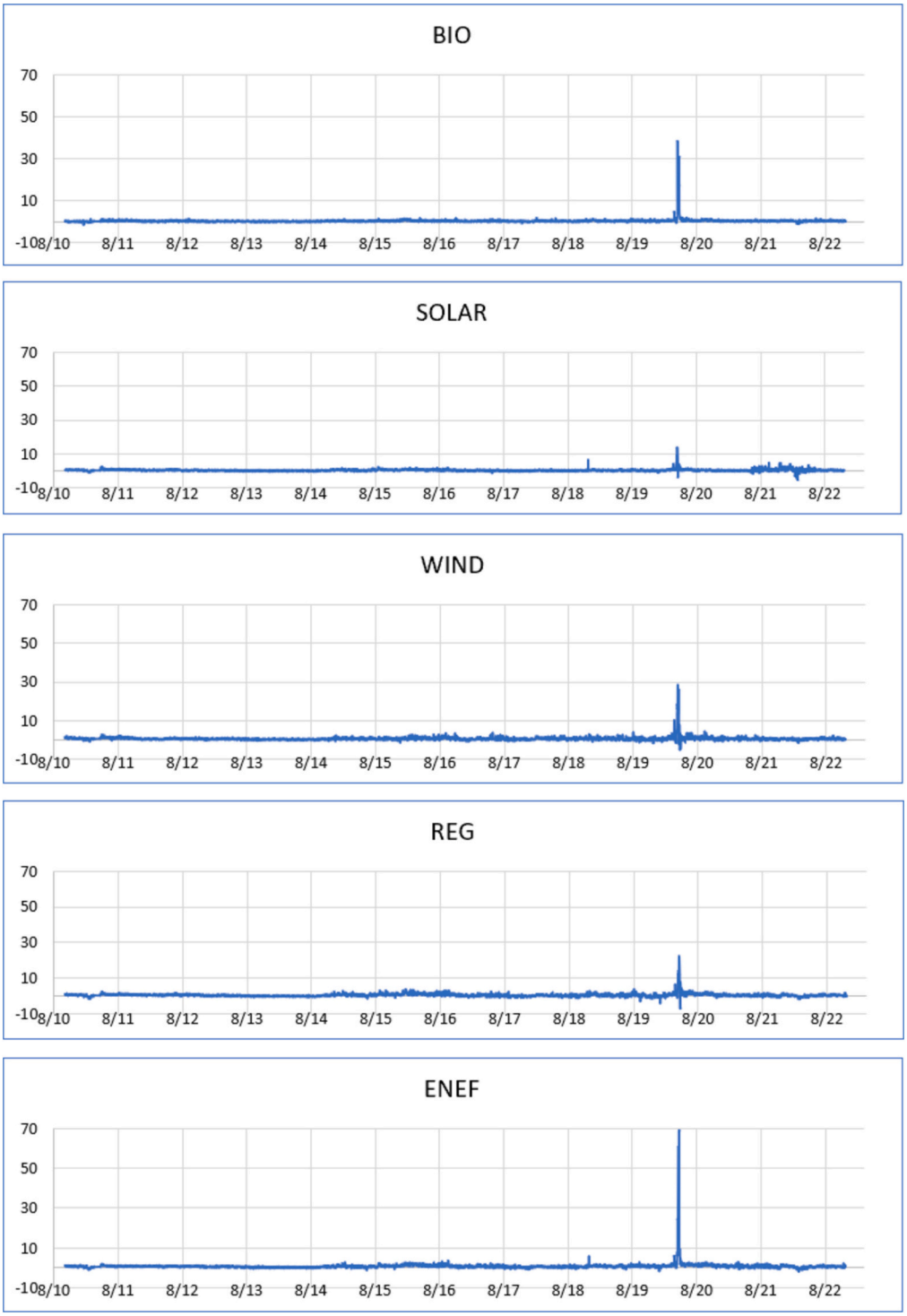

Fig. 6. Optimal hedge ratio (Minimum variance portfolio).
Note: BIO, SOLAR, WIND, REG, and ENEF represent the NASDAQ OMX Biofuel, Wind, Solar, Renewable Energy Generation, and Energy Efficiency Indexes.

the utility function and hedgers' risk aversion.

Under the minimum variance hedging strategy, the objective is to minimize risk regardless as to the return and investors are subject to infinite risk aversion. The optimal hedge ratio is:

$$\beta_t = \frac{Cov_{Oil,Clean,t}}{Var_{Clean,t}} \tag{21}$$

where $Cov_{Oil,Clean,t}$ denotes the realized covariance between the oil and clean energy markets and $Var_{Clean,t}$ denotes the variance of the clean energy markets.

Note that the minimum variance strategy assumes that returns are normally distributed and investors are infinitely risk averse (Cotter and Hanly, 2015). Thus, this strategy may produce suboptimal asset allocations if either of the assumptions are violated. Following Patton (2004), we adopt a utility-based hedging measure as an alternative. The objective is to choose a hedge ratio to maximize investors' utility, which depends upon their risk preference. To accommodate the effect of higher-order moments on expected utility, we adopt the exponential

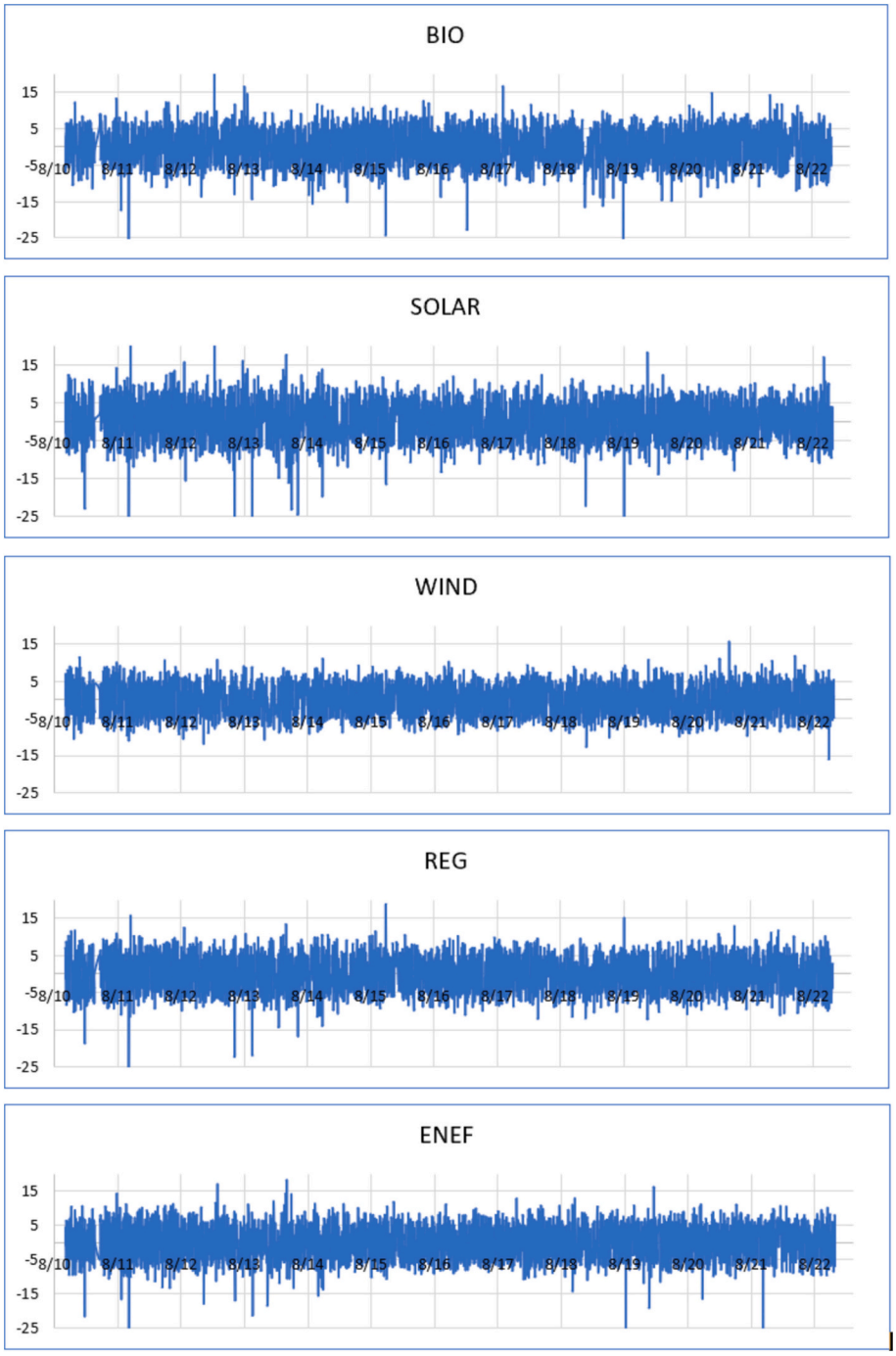

Fig. 7. Optimal hedge ratio (Exponential utility - λ = 10).
Note: BIO, SOLAR, WIND, REG, and ENEF represent the NASDAQ OMX Biofuel, Wind, Solar, Renewable Energy Generation, and Energy Efficiency Indexes.

utility function:

$$U(W_t) = -\lambda e^{-W_t/\lambda} \tag{22}$$

where W_t denotes investors' wealth and λ denotes their risk aversion.[5] We consider two alternative values for λ, specifically, $\lambda = 10$ and $\lambda = 5$, to account for different levels of risk aversion. The optimal hedging ratio for an investor with exponential utility can be estimated by choosing β_t that maximizes the following expression:

$$E[W_t] - \frac{1}{2\lambda} Var(W_t) + \frac{1}{6\lambda^2} Skew(W_t) - \frac{1}{24\lambda^3} Kurt(W_t) \tag{23}$$

where $E[W_t]$ is the expected return. $VAR(W_t)$, $Skew(W_t)$, and $Kurt(W_t)$ are the variance, skewness, and kurtosis of the portfolio and are estimated based on realized higher-order moments using five-minute

[5] Higher λ corresponds to higher risk aversion.

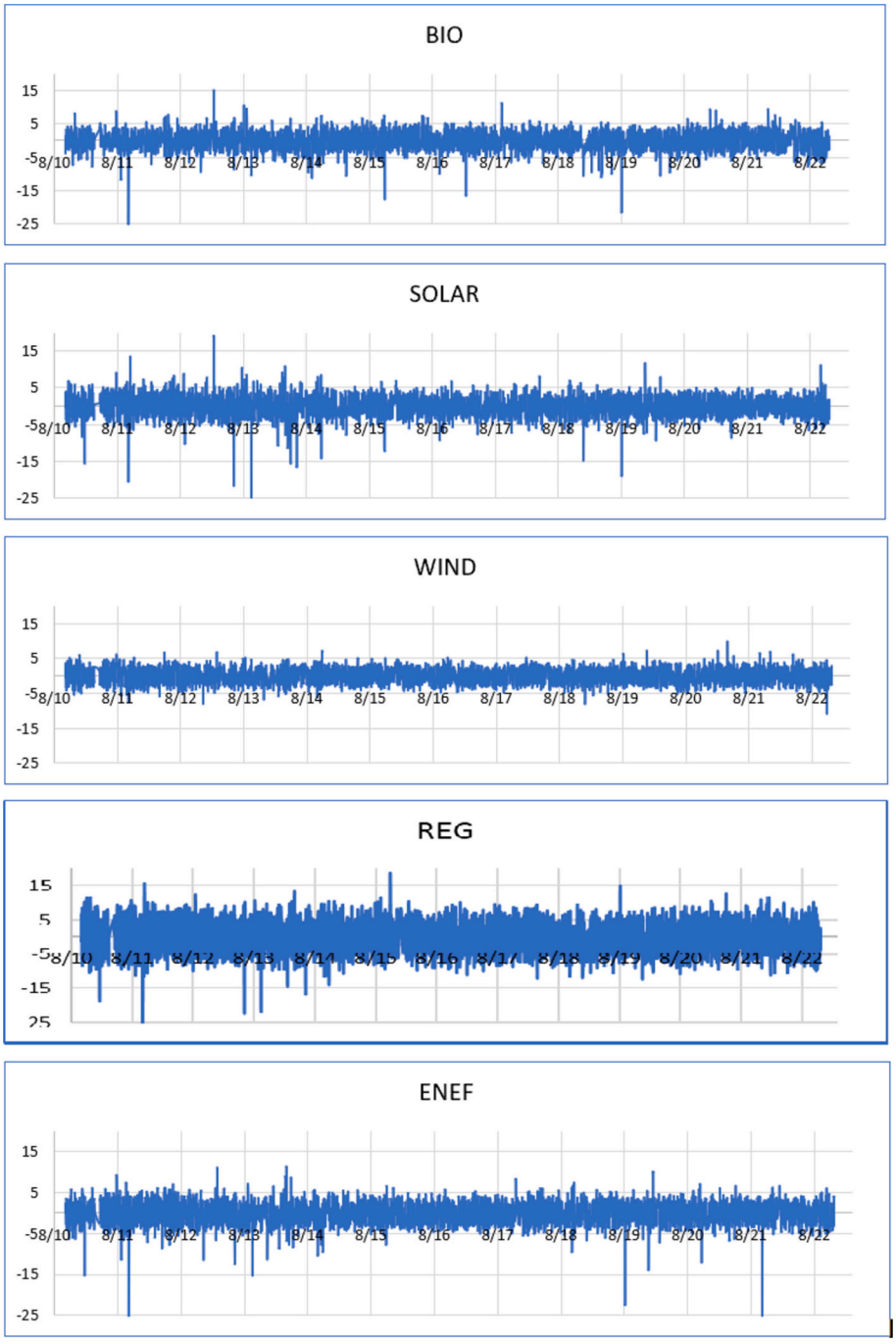

Fig. 8. Optimal hedge ratio (Exponential utility $\lambda = 5$).
Note: BIO, SOLAR, WIND, REG, and ENEF represent the NASDAQ OMX Biofuel, Wind, Solar, Renewable Energy Generation, and Energy Efficiency Indexes.

Table 4
Portfolio performance metrics.

	Portfolio strategies			
Portfolio	Unhedged	Minimum Variance	Exponential Utility ($\lambda = 10$)	Exponential Utility ($\lambda = 5$)
(OIL, BIO)				
Mean	–	0.3126	0.0167	−0.0848
SD	–	1.0904	5.2755	2.9977
HE	–	**0.3462**	−2.2995	−0.7617
Exponential (lambda = 10)	0.0014	−0.2616	**0.4053**	−0.2108
Exponential (lambda = 5)	−0.0006	−2.0170	−6.3080	**0.6700**
Information Ratio	0.4098	0.5024	**3.674**	3.516
(OIL, SOLAR)				
Mean	–	0.3743	0.0377	−0.0076
SD	–	0.6314	5.5974	3.1454
HE	–	**−0.1352**	−3.0513	−1.0303
Exponential (lambda = 10)	0.0014	−0.0003	**0.7505**	0.0955
Exponential (lambda = 5)	−0.0006	−0.0240	−5.9270	**1.2858**
Information Ratio	0.4098	0.5568	3.717	**3.858**
(OIL, WIND)				
Mean	–	0.4598	−0.0072	−0.0159
SD	–	1.1611	4.4808	2.3353
HE	–	**0.0230**	−1.1298	−0.2919
Exponential (lambda = 10)	0.0014	−0.1710	**0.1477**	−0.1843
Exponential (lambda = 5)	−0.0006	−1.2857	−9.3510	**0.1191**
Information Ratio	0.4098	0.4777	**3.989**	3.411
(OIL, REG)				
Mean	–	0.6875	−0.0702	−0.0767
SD	–	0.9476	5.0539	2.7102
HE	–	**0.0664**	−0.7489	−0.2099
Exponential (lambda = 10)	0.0014	−0.0196	**0.2445**	−0.0804
Exponential (lambda = 5)	−0.0006	−0.1820	−5.8670	**0.3357**
Information Ratio	0.4098	0.4996	**4.137**	3.156
(OIL, ENEF)				
Mean	–	0.6953	0.0067	−0.0637
SD	–	1.9684	5.4068	3.0163
HE	–	**0.2254**	−1.2337	−0.4124
Exponential (lambda = 10)	0.0014	−1.9207	**0.7081**	0.5044
Exponential (lambda = 5)	−0.0006	−14.7741	−0.1941	**1.2898**
Information Ratio	0.4098	0.2266	**3.809**	3.147

Note: Each panel presents the performance metrics for a portfolio of a long position in oil and a short position in the clean energy markets. Four investment scenarios are considered: Unhedged, Minimum Variance, Exponential Utility with a risk aversion parameter of 10, and Exponential Utility with a risk aversion parameter of five. Mean, SD, and HE are the average hedge ratio, the standard deviation of hedge ratios, and hedging effectiveness. The rows "Exponential ($\lambda = 10$)" and "Exponential ($\lambda = 5$)" present the utility values of the exponential utility function under each investment strategy for risk aversion parameters of 10 and five. The row "Information Ratio" presents the information ratio, which is the ratio between portfolio returns and the standard deviation. BIO, SOLAR, WIND, REG, and ENEF represent the NASDAQ OMX Biofuel, Wind, Solar, Renewable Energy Generation, and Energy Efficiency Indexes.

Table 5
Expected utility gain under alternative hedging strategies.

		Hedging strategies	
Portfolio	λ	Minimum Variance	Exponential Utility
(OIL, BIO)	10	−0.2630	0.4039
	5	−2.0163	0.6706
(OIL, SOLAR)	10	−0.0018	0.7490
	5	−0.0234	1.2865
(OIL, WIND)	10	−0.1724	0.1463
	5	−1.2851	0.1198
(OIL, REG)	10	−0.0211	0.2430
	5	−0.1814	0.3363
(OIL, ENEF)	10	−1.9222	0.7067
	5	−14.7735	1.2904

Note: The table presents the expected utility gain of the minimum variance hedge ratios and the exponential utility hedge ratios, compared to the utility of an unhedged position in oil, across different risk aversion parameters (λ). BIO, SOLAR, WIND, REG, and ENEF represent the NASDAQ OMX Biofuel, Wind, Solar, Renewable Energy Generation, and Energy Efficiency Indexes.

Table 6
Minimum connectedness portfolio performance indicators.

Table 6.1. Portfolio return summary statistics.

Portfolio	Mean Return	SD of Return	Info. Ratio
Oil (Unhedged)	0.00200	0.06990	0.02864
MCP (Realized Volatility)	0.00228	0.05967	0.03823
MCP (Jump component of realized volatility)	0.00113	0.03101	0.03643
MCP (Realized Skewness)	0.00064	0.02017	0.03192
MCP (Realized Kurtosis)	0.00064	0.01962	0.03264

Table 6.2 Average weights of oil and hedging effectiveness

Portfolio	Mean weight	SD of weight	Hedging effectiveness (%)
Oil (Unhedged)	1.00	0.00	0.00
MCP (Realized Volatility)	0.37	0.29	0.27
MCP (Jump component of realized volatility)	0.14	0.15	0.80
MCP (Realized Skewness)	0.22	0.05	0.92
MCP (Realized Kurtosis)	0.20	0.04	0.92

Note: The table presents the performance indicators of an unhedged position in oil price, and the minimum connectedness portfolio in realized volatility, the jump component of volatility, realized skewness, and realized kurtosis. Table 6.1 presents the portfolio returns, the standard deviation of returns, and the information ratios. Table 6.2 reports the average weight of oil in each portfolio and the hedging effectiveness provided by each portfolio against variations in oil prices.

intraday data.[6]

Figs. 6–8 plot the time-varying optimal hedge ratios under the minimum variance and the exponential utility-based strategies from 2010 to 2022. Overall, we find that the exponential utility based hedge ratios are more variable than the minimum variance hedge ratios. This can be explained by the fact that higher-order moments are included in the exponential utility function while they are not included in the minimum variance strategy. Since these higher-order moments capture additional risks, such as asymmetry risks (measured by skewness) and fat tail risks (measured by kurtosis), this requires more frequent adjustments of the optimal hedge ratios. Under the minimum variance hedging strategy (Fig. 6), we find the biggest adjustment in the hedging portfolios during the Covid-19 pandemic period and Russia-Saudi Arabia oil price war in 2020. The adjustment is the most pronounced for the Renewable Energy Generation stocks with the optimal hedge ratio increased significantly to 70 %. The hedge ratios increase to 40 % and 30 %, respectively, for Biofuel and Wind stocks and 20 % and 15 %, respectively, for Solar and Energy Efficiency stocks during the same period. While in other periods, the hedge ratios remain relatively stable across all clean energy sectors. Under the utility-based hedging strategy (Figs. 7 and 8), hedge ratios reflect the short-term risks better with the inclusion of higher-order moments. Optimal hedge ratios switch between positive and negative values throughout the sampling period across all energy sectors. In other words, to effectively use clean energy stock to hedge oil price risks, it is necessary to actively switch between long and short positions. The switches between the long and short positions are stronger and more active when Biofuel, Solar, Renewable Energy Generation, and Energy Efficiency stocks are included in the hedging positions against the oil price risk and become weaker when Wind stocks are included in the hedging positions. The switches between the long and short positions also appear to be stronger when investors are more risk averse as shown in Fig. 7.

Table 4 summarizes the performance metrics for alternative portfolio strategies. The bolded numbers indicate the best performing portfolio for a given performance metric. In terms of the hedging effectiveness, defined as the percentage of volatility reduction by investing in the portfolio compared to an unhedged oil position, the minimum variance strategy offers the highest hedging effectiveness compared to the utility-based strategies. This is in line with the fact that investors who choose the minimum variance strategy are assumed to be extremely risk averse. Therefore, they are willing to minimize risk regardless of the returns. However, for investors who are less risk averse, the utility-based strategy offers higher utility implying that the minimum variance strategy may lead to sub-optimal asset allocations in these scenarios. Specifically, the information ratios show that the exponential utility-based portfolios offer better risk-return trade-offs than the minimum variance portfolio. For example, in the (OIL, BIO) portfolio, information ratios for the exponential utility portfolios are 3.674 ($\lambda = 10$) and 3.516 ($\lambda = 5$), which are significantly higher than those for the unhedged and minimum variance portfolio (0.4098 and 0.5024). Similar observations can be made for other oil-clean energy stock pairs. Since the exponential utility-based portfolios incorporate information about investors' risk aversion and higher-order moment movements of asset returns, our results illustrate the usefulness of considering higher-order moments in asset allocation strategies.

In terms of the utility derived from each hedging strategy, we find that investors can benefit from switching to a utility-based hedge. For example, the utility from the exponential utility function for an investor with a risk averse parameter of $\lambda = 10$ is 0.4053 in the (OIL, BIO) portfolio. Similarly, investors with a smaller risk aversion ($\lambda = 5$) also derive larger utility from the exponential utility portfolio (0.6700). These are significantly higher than the utility derived from the unhedged portfolio (0.0014 and $-$ 0.0006 for $\lambda = 10$ and $\lambda = 5$, respectively), or from the minimum variance portfolio ($-$0.2616 and $-$ 2.0170 for $\lambda = 10$ and $\lambda = 5$, respectively). Similar observations can be made for other oil-clean energy stock pairs.

Table 5 presents the expected utility gain of the portfolios under alternative hedging strategies compared to an unhedged position in oil. The table reports that the minimum variance portfolios yield smaller utility than the unhedged position since the expected utility gain from this strategy is negative for all asset pairs. Additionally, the loss in utility from the minimum variance portfolio is larger for $\lambda = 5$ than for $\lambda = 10$. As λ indicates the level of risk aversion, the results from Table 5 suggests that investors with less risk aversion (smaller λ) will suffer from larger utility loss compared to other investors from the minimum variance portfolio. Conversely, the utility gain for investors with less risk aversion is larger in the exponential utility hedging strategy. This is illustrated by the fact that the utility gain for investors with $\lambda = 5$ is larger than that for $\lambda = 10$ across all asset pairs in Table 5.

To demonstrate the utility gain from switching to a utility-based hedging strategy further, we compare the utility gain from the minimum variance and exponential utility hedge ratios during the post-COVID-19 period in Table B.1. We define the post-COVID period as the period after January 1, 2020 until the end of our sampling period. Our results indicate that while the utility gain from the exponential utility hedging strategy is still positive across all asset pairs, the minimum variance hedge ratios lead to a larger reduction in utility during the post-COVID-19 period. Thus, our results indicate the usefulness of the exponential utility hedging strategies during the most recent economic crisis for investors who are not infinitely risk averse.

5.2. Minimum connectedness portfolios

To demonstrate the usefulness of the higher-order moments in oil-clean energy portfolio management further, we construct four alternative portfolios based on the TVP-VAR connectedness network in Section 4.2. Specifically, we construct the minimum connectedness portfolios (MCPs) in realized volatility, the jump component of realized volatility, realized skewness, and realized kurtosis. In these portfolios, the weights of the assets vary according to their connectedness with other variables in each higher moment. We first calculate the pairwise connectedness index in higher moments between two assets as follows (Tiwari et al., 2022; Broadstock et al., 2022):

$$PCI_{ij,t} = 2^{*}\frac{jSOT_{ij,t} + jSOT_{ji,t}}{jSOT_{ii,t} + jSOT_{ji,t} + jSOT_{ij,t} + jSOT_{jj,t}} \tag{24}$$

By construction, $PCI_{ij,t} \in [0, 1]$ and captures the level of connectivity between the variables. Let PCI_t be the pairwise connectedness matrix on day t, whose ij-th element is $PCI_{ij,t}$. Let I be the $n \times n$ identity matrix. The portfolio weights of the variables in the system are:

$$w = \frac{PCI_t^{-1} * I}{I * PCI_t^{-1} * I} \tag{25}$$

Table 6 presents a summary of the performance indicators of an unhedged position in oil price and the minimum connectedness portfolios (MCPs) in each higher moment (i.e., realized volatility, the jump component of realized volatility, realized skewness, and realized

[6] These are given by: $Var(W_t) = Var_{Oil,t} - 2^{*}\beta_t Cov_{Oil,Clean,t} + \beta^2 Var_{Clean,t}$

$$\boldsymbol{Skew}(\boldsymbol{W}_t) = \boldsymbol{Skew}_{Oil,t} - \boldsymbol{\beta}_t^3 \boldsymbol{Skew}_{Clean,t} + \mathbf{3}(\boldsymbol{\beta}^2 - \boldsymbol{\beta})\boldsymbol{CoSkew}_{Oil,Clean,t}$$

$$\boldsymbol{Kurt}(\boldsymbol{W}_t) = \boldsymbol{Kurt}_{Oil,t} + \boldsymbol{\beta}_t^4 \boldsymbol{Kurt}_{Clean,t} - \mathbf{4}(\boldsymbol{\beta}_t^3 + \boldsymbol{\beta}_t)\boldsymbol{CoKurt}_{Oil,Clean,t} + \mathbf{6}\boldsymbol{\beta}^4 \boldsymbol{Cov}_{Oil,Clean,t}$$

where $Var_{j,t}, Skew_{j,t}, and\ Kurt_{j,t}$ stand for the variance, skewness, and kurtosis of asset j on day t. $Cov_{i,j,t}, CoSkew_{i,j,t}, and\ CoKurt_{i,j,t}$ stand for the co-variance, co-skewness, and co-kurtosis between assets i, j on day t. We estimate $Var_{j,t}, Skew_{j,t}, Kurt_{j,t}, Cov_{i,j,t}, CoSkew_{i,j,t}, and\ CoKurt_{i,j,t}$ by calculating the realized measures using the five-minute intraday data following Nekhili and Bouri (2023). See Nekhili and Bouri (2023) for more details.

kurtosis). Table 6.1 presents the portfolio returns, standard deviation of returns, and information ratios. Table 6.2 provides the average weight of oil in each portfolio and the hedging effectiveness provided by each portfolio against variations in oil prices. The table indicates that the information ratio on the MCPs is higher than that for oil price implying that the MCPs provide better risk-return tradeoffs compared to an unhedged position in oil. Additionally, the hedging effectiveness of the MCPs are positive. Thus, the MCPs offers some hedging benefits against an unhedged position in oil. However, we find the hedging effectiveness of the MCPs to be quite small. Thus, this corroborates our findings in Section 5.1 that while higher-order moment portfolio strategies offer smaller hedging effectiveness, they offer better risk-return trade-offs. Investors who are not infinitely risk-averse would prefer higher-order moment portfolio strategies, while infinitely risk-averse investors would prefer the minimum variance hedging strategy.

5.3. Robustness analyses

To test the robustness of our analysis, we consider alternative forecast horizons of five days (a trading week - Fig. A.1), 20 days (a trading month - Fig. A.2), and 60 days (a trading quarter - Fig. A.3) and alternative lag structures of the TVP-VAR model (Figs. A.4-A.5). We also consider alternative prior models, such as the Bayesian and the uninformative priors (Figs. A.6-A.7), and alternative forgetting factors (Figs. A.8-A.9). Next, we test the robustness of our results using alternative connectedness models that include the original models of Diebold and Yilmaz (2009, 2012, 2014) with a 200-day rolling window, the joint connectedness model with a 200-day rolling window of Lastrapes and Wiesen (2021) and the TVP-VAR model of Antonakakis et al. (2020) (Figs. A.10-A.12).[7] We present the results of these alternative models in Appendix A. Overall; we find that our results are consistent with the results of these alternative models.

Next, we test the robustness of our results under the R2 model-free connectedness model of Balli et al. (2023). This model is a measure of unconditional connectedness, built solely upon variance and covariance, and allows separating total connectedness into contemporaneous and lagged connectedness. Fig. A.13 presents the total connectedness indexes under this model. We find that the contemporaneous and lagged connectedness indexes tend to be in the same direction, and the contemporaneous connectedness are typically larger than the lagged connectedness. Because the contemporaneous effect plays a larger role in explaining the spillovers across the variables, we will leave the exploration of the lagged effects for future research. Finally, we test the robustness of our results using the quantile vector autoregression model for the median quantile with a rolling window of 200 days following Ando et al. (2022). The benefit of using a quantile regression is that it makes no assumption about the parametric form of the distribution of the response variables nor does it assume that the variance of the response variables is constant. Our results in Fig. A.14 of the appendix indicate that the connectedness indexes under the quantile connectedness model are similar to those obtained from our TVP-VAR model. However, a drawback of the quantile connectedness model is that it relies on the selection of an arbitrary rolling window. Additionally, it is computationally unable to estimate the connectedness indexes for the jump component of volatility. Thus, we rely on the TVP-VAR model for our main analysis and present the quantile connectedness results as robustness checks.

In addition, we consider the utility-based hedge ratios under alternative utility functions, such as the quartic, logarithmic, and hyperbolic power utility. These utility functions are alternative ways to incorporate all of the moments of the distributions into hedging strategy constructions (Brooks et al., 2012). Tables B.2-B.3 of Appendix B present the utility gains from utilizing the utility-based hedge ratios across the alternative utility functions. As a point of reference, we also include the utility gains from using the quadratic utility function that takes into account the first and second moments of the return distributions. Our results in Tables B.2-B.3 indicate that our previous conclusions are still valid. Specifically, investors who are not infinitely risk averse can enjoy potential utility gains from switching to utility-based hedging strategies, especially during the post-COVID-19 period. This highlights the relevance of considering higher moments in portfolio management.

Finally, we consider the performance of the minimum higher moment connectedness portfolio during the post-COVID-19 period. Our results in Table C.1. of the appendix suggest that the information ratio of the minimum connectedness portfolio based on realized volatility and its jump component is larger than that of the unhedged position in oil. However, using other higher-order moments to construct the minimum connectedness portfolio leads to a slight decrease in the information ratio during this period. This reflects the fact that the energy market experiences a number of shocks during this period, such as the COVID-19 financial crisis, the Russia-Saudi Arabia oil price war, and the Russia-Ukraine war. This suggests that other hedging strategies may be useful to hedge oil price shocks during crisis periods. This result is consistent with Nekhili and Bouri (2023) who find that higher-order moment hedging strategies do not improve the hedging performance of gold against oil prices during the COVID-19 period. In addition, we test the ex-ante or out-of-sample performance of the higher-order minimum connectedness strategies. Specifically, for each period, we first calculate the one-step-ahead pairwise connectedness index matrix that is then used to calculate the one-step-ahead minimum connectedness portfolio and portfolio performance. We obtain 2000 one-step-ahead minimum connectedness portfolios from this procedure. Tables C.2 in Appendix C presents the estimation results. We find that the out-of-sample higher-moment portfolios are very similar to the ex-post higher-moment portfolios using the full sample data in Table 6. Moreover, we compare the out-of-sample higher-order minimum connectedness portfolios in Table C.2 with the out-of-sample minimum quantile connectedness portfolios. The quantile-based portfolios are based on the results of the quantile connectedness models at the extreme upper and lower quantiles (i.e., the 5th and 95th quantiles of asset returns). Table C.3 presents the estimation results. We find that the portfolio performances are comparable between the higher-moment portfolios (Table C.2) and the quantile-based portfolios (Table C.3). However, the higher-moment portfolios, particularly the portfolios constructed from the 3rd and 4th moments, offer better risk-return trade-offs and hedging effectiveness compared to the quantile portfolios. We believe both the quantile and higher-moment portfolios offer different insights into asset behavior and are suitable for investors with different risk appetites. Specifically, the quantile-based portfolios focus on one specific region of the return distributions and depend upon the choices of the quantiles. The higher-moment-based portfolios are realized measures and focus on the shapes of the return distributions (e.g., asymmetry, tail thickness). We leave further explorations of how to combine the quantile and higher-moment methods in portfolio management strategies for future research.

6. Conclusions

In this paper, we study the connectedness between clean energy stock and oil prices at higher-order moments including realized volatility, jumps, realized skewness, and realized kurtosis, and demonstrate the usefulness of considering higher-order moments in a clean energy-oil portfolio. Our initial analysis on static higher-order moment connectedness between clean energy stock and oil prices shows that the clean energy sectors and oil market are highly connected at all higher-order moments. We find that the connectedness between clean energy and oil markets are moment dependent, and the shock transmitter or recipient roles played by each clean energy sector and oil market also vary across different moments. Our further analysis regarding the time

[7] Our results for the rolling-window models are consistent across other choices of the rolling windows (150 or 250 days).

dynamic higher-order moment connectedness between clean energy stock and oil prices reveals that the connectedness is time varying and turbulent time periods are associated with stronger connectedness between the clean energy and oil markets.

To explore the time varying behaviors further, we study the day-of-the-week patterns of higher-order moment connectedness. We find that connectedness intensifies from Mondays to Fridays due to the incorporation and accumulation of news information throughout the trading week. The day-of-the-week patterns appear to be the opposite during low vs. high uncertainty periods indicating that the connectedness between the clean energy and oil markets is conditional upon the market states and uncertainty. We next employ a Markov switching regression model to establish a formal relationship between higher-order moment connectedness and economic, political, and financial market uncertainty. Our results suggest that oil and stock market volatility are the main drivers of higher-order moment connectedness, while economic policy uncertainty and geopolitical risk play more modest roles.

We contribute to the literature by unraveling how the oil and clean energy markets are related to each other across higher-order moments, thereby capturing their spillovers in asymmetry risks, jump risks, and fat tail risks. Our findings of the heterogeneous connectedness between the oil and clean energy markets across the moments highlight the relevance of considering higher-order moments in investment portfolio design. The above findings have important implications for investors in portfolio allocation decisions. As an important extension, we conduct formal tests to investigate how clean energy stocks can be used to hedge oil price risks. We consider a minimum variance investment strategy that seeks to minimize risk regardless as to the return for risk averse investors, a utility-based investment strategy whose goal is to maximize investors' utility by considering investors' risk preference and higher-order moment movements of asset returns, and a minimum connectedness portfolio in higher moments that aims to minimizes the pairwise higher-moment connectedness across variables. Our results show that the minimum variance strategy offers the highest hedging effectiveness compared to the utility-based strategy. However, the utility-based strategy and the minimum connectedness portfolios in higher moments offer higher utility and better risk-return trade-offs than the minimum variance portfolio corroborating the usefulness and importance of considering higher-order moments in asset allocation strategies.

CRediT authorship contribution statement

Wei Hao: Writing – review & editing, Writing – original draft, Validation, Project administration, Methodology, Formal analysis, Conceptualization. **Linh Pham:** Writing – review & editing, Writing – original draft, Validation, Software, Methodology, Formal analysis, Conceptualization.

Declaration of competing interest

None.

Appendix A. Robustness analyses of the connectedness models

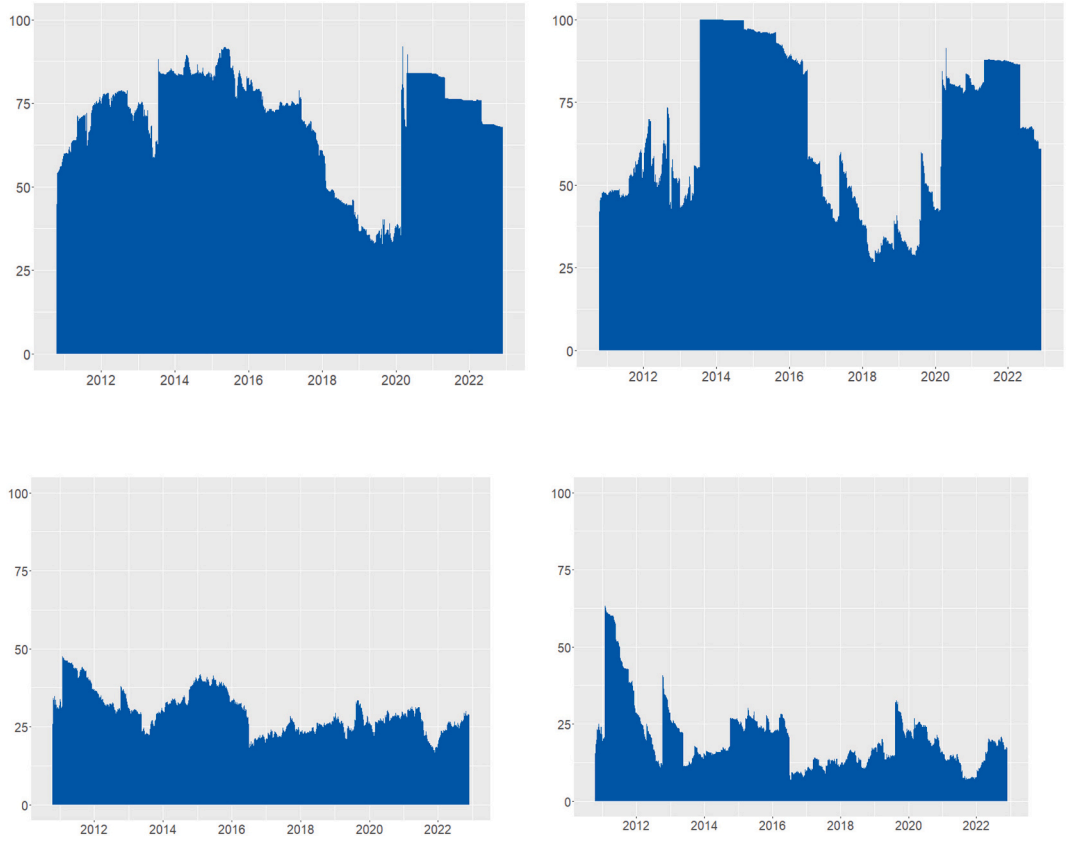

Fig. A.1. Total connectedness indexes – TVP-VAR Extended Joint Connectedness Model with a 5-day forecast horizon.
Note: The figure presents the TCI obtained from using a forecast horizon of 5 days in our main empirical model.

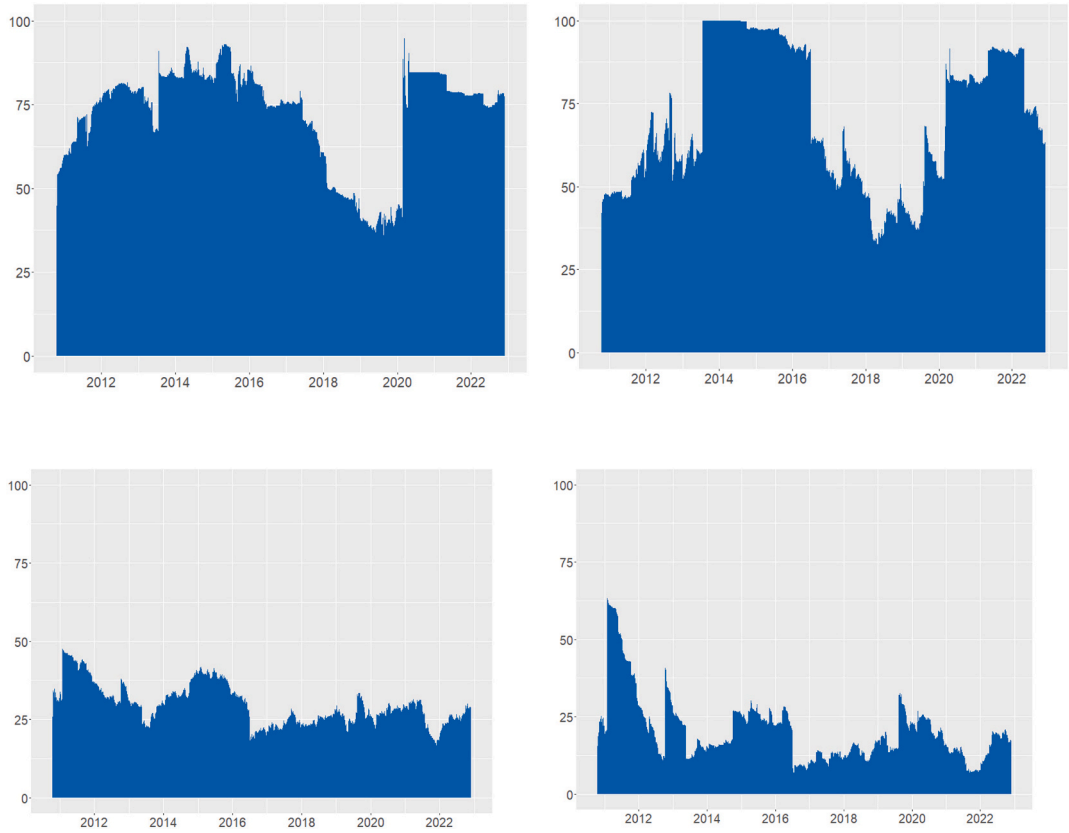

Fig. A.2. Total connectedness indexes – TVP-VAR Extended Joint Connectedness Model with a 20-day forecast horizon.
Note: The figure presents the TCI obtained from using a forecast horizon of 20 days in our main empirical model.

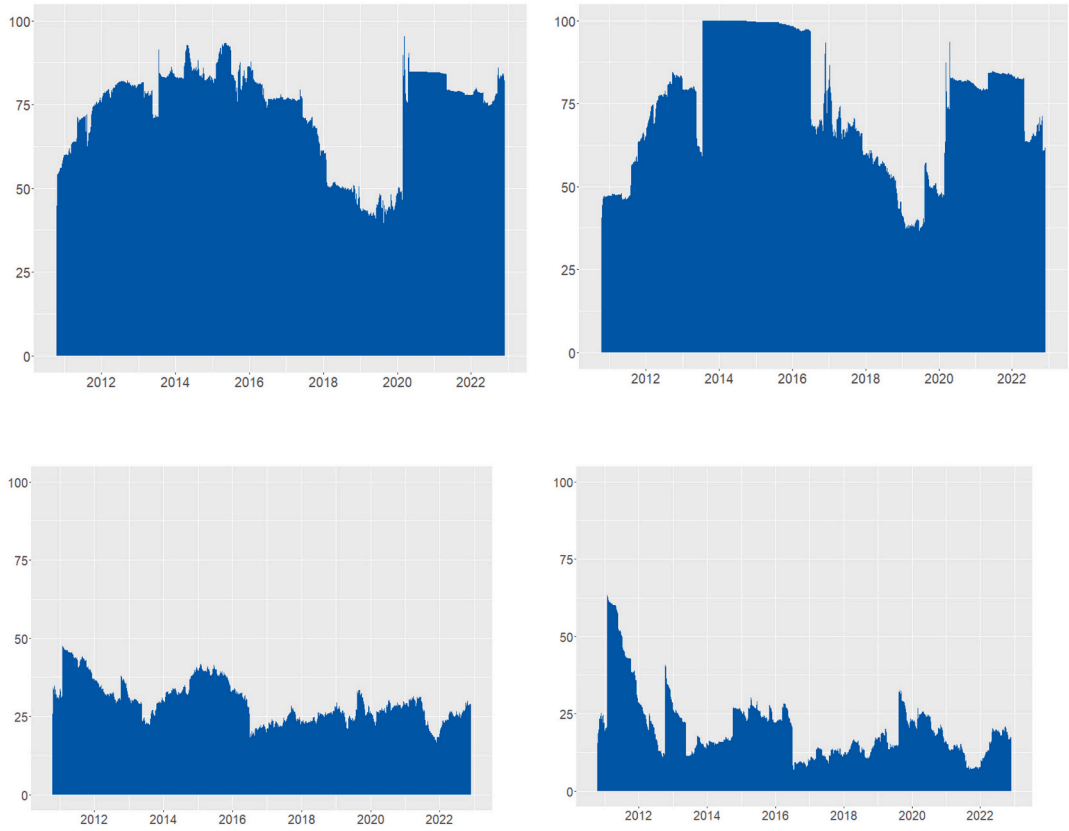

Fig. A.3. Total connectedness indexes – TVP-VAR Extended Joint Connectedness Model with a 60-day forecast horizon.
Note: The figure presents the TCI obtained from using a forecast horizon of 60 days in our main empirical model.

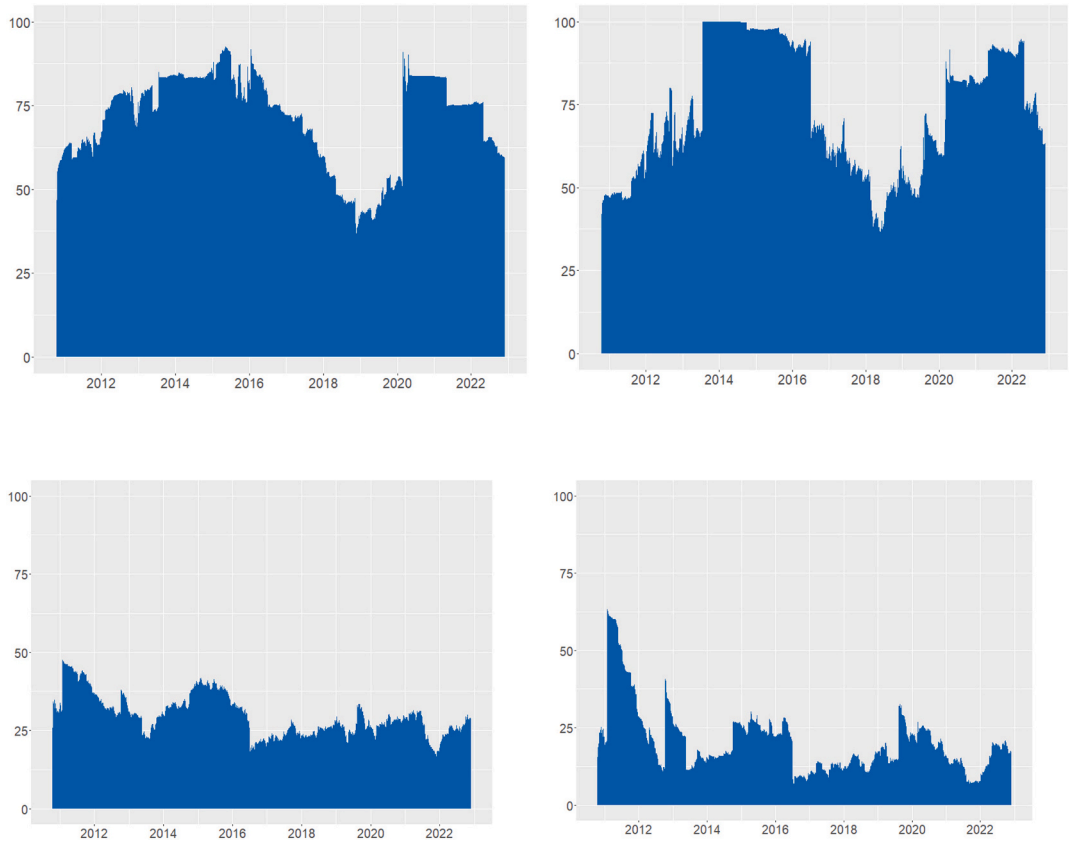

Fig. A.4. Total connectedness indexes – TVP-VAR Extended Joint Connectedness Model with a lag length of 1 in the TVP-VAR regression.
Note: The figure presents the TCI obtained from using a lag length of 1 in our main empirical model.

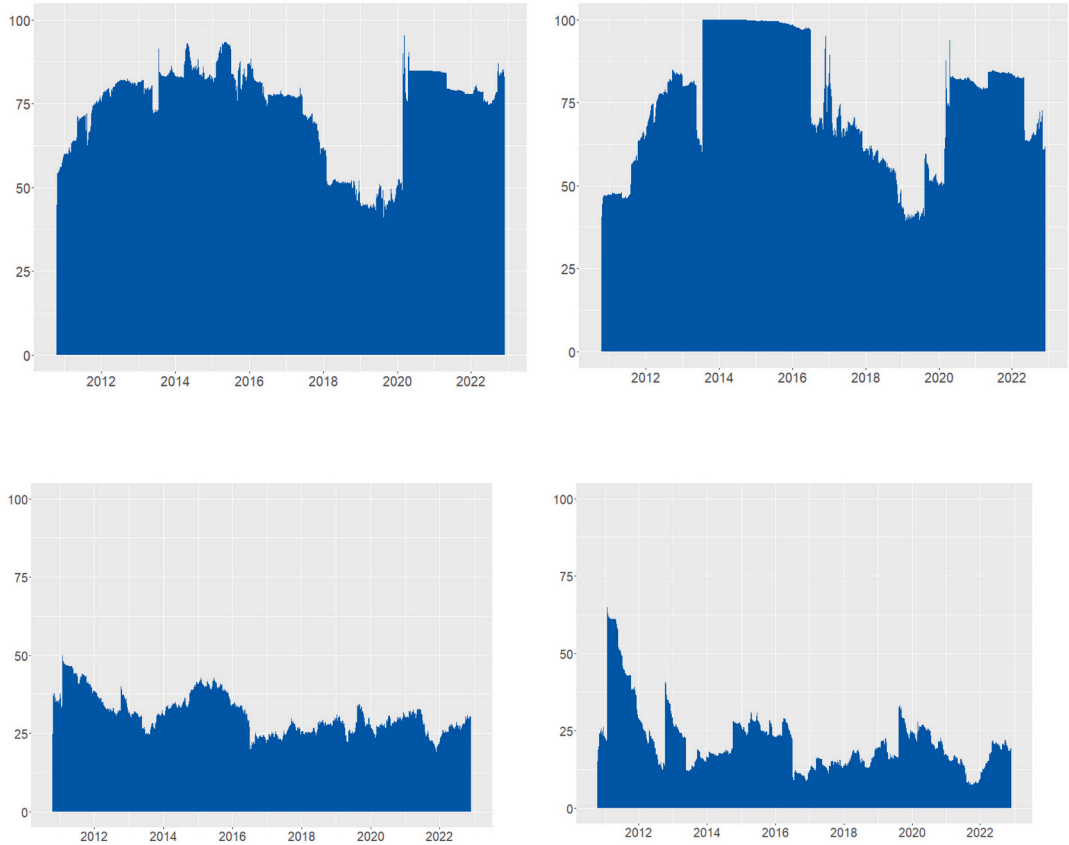

Fig. A.5. Total connectedness indexes – TVP-VAR Extended Joint Connectedness Model with a lag length of 2 in the TVP-VAR regression.
Note: The figure presents the TCI obtained from using a lag length of 2 in our main empirical model.

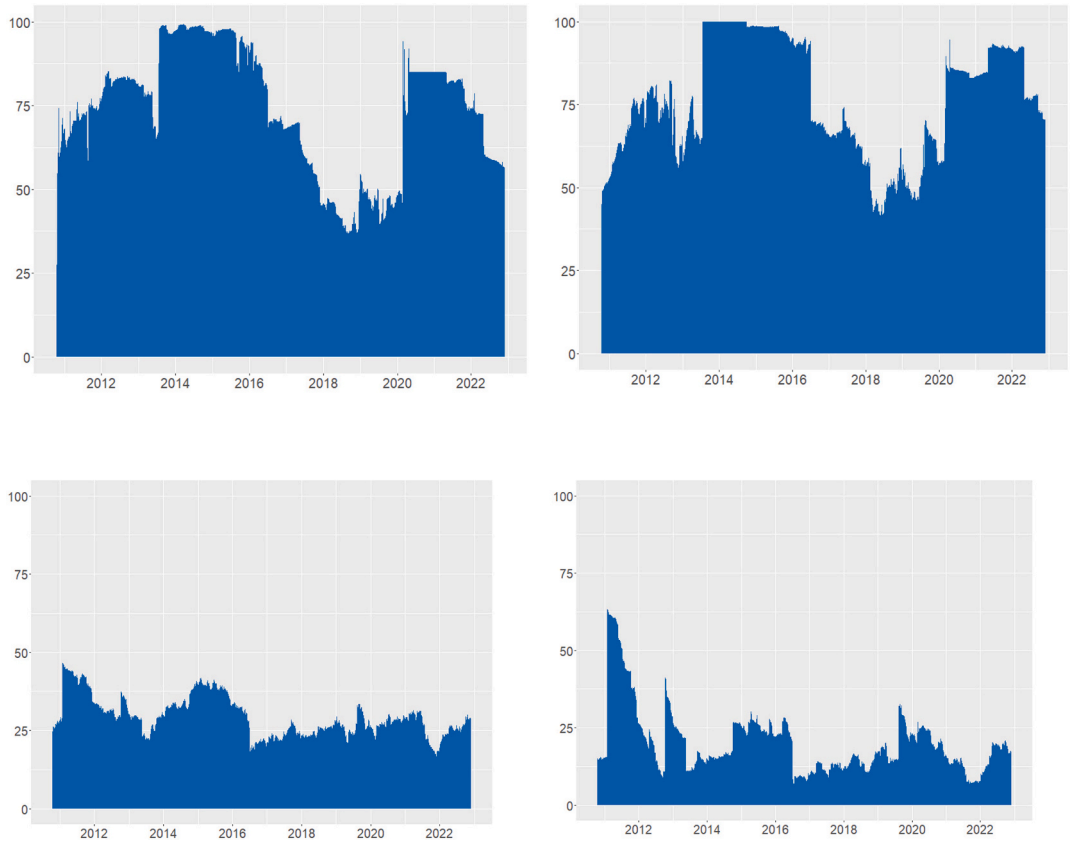

Fig. A.6. Total connectedness indexes – TVP-VAR Extended Joint Connectedness Model with Bayesian Priors.
Note: The figure presents the TCI obtained from using the Bayesian priors in our main empirical model.

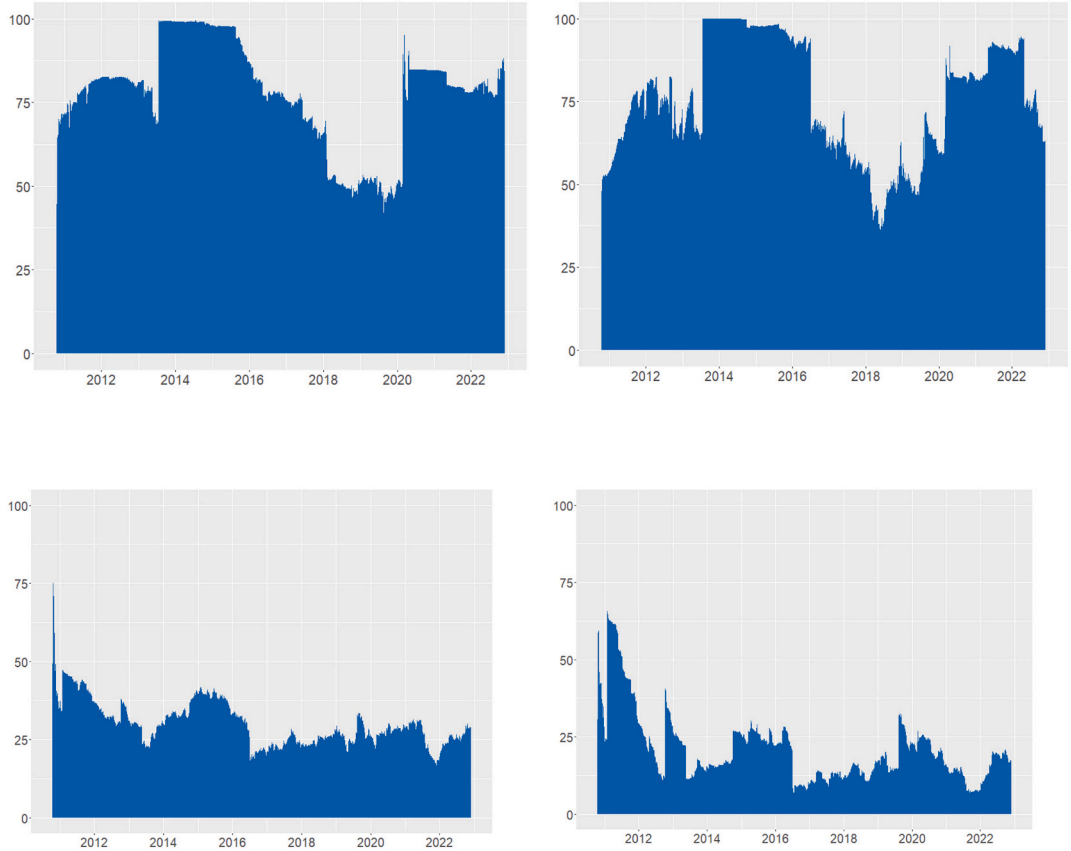

Fig. A.7. Total connectedness indexes – TVP-VAR Extended Joint Connectedness Model with Uninformative Priors.
Note: The figure presents the TCI obtained from using the uninformative priors in our main empirical model.

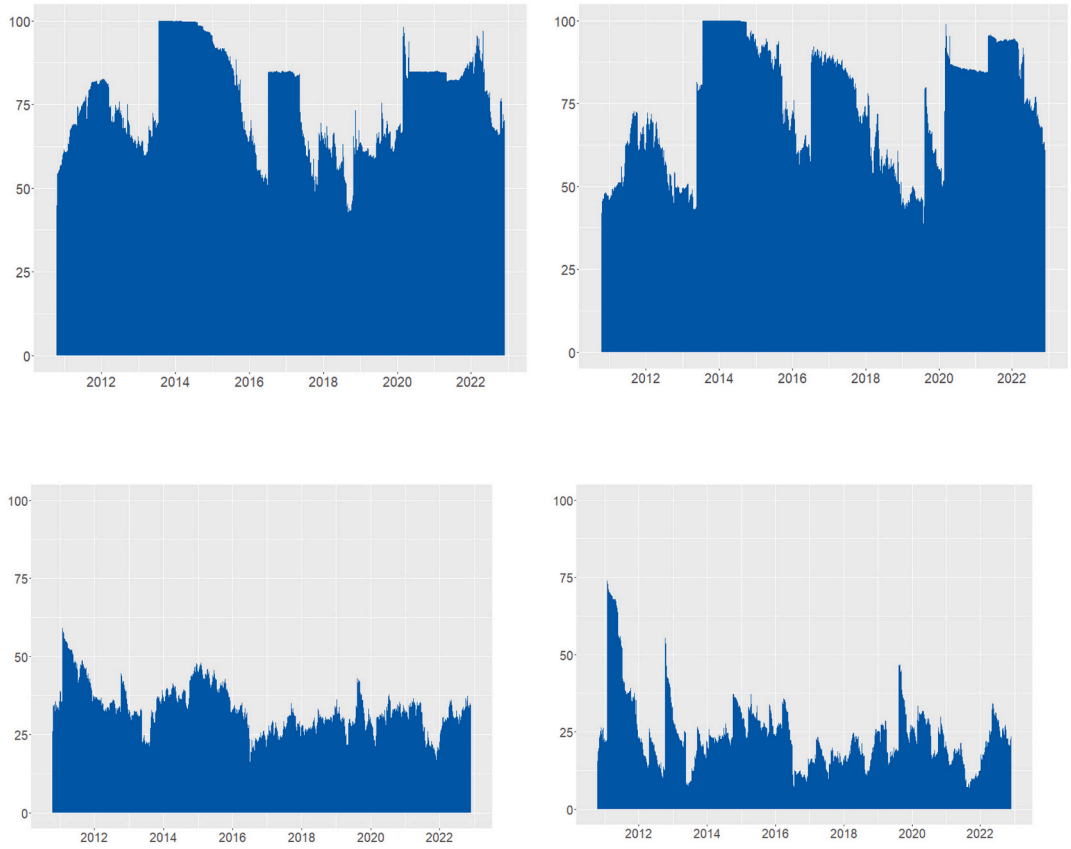

Fig. A.8. Total connectedness indexes – TVP-VAR Extended Joint Connectedness Model with a 0.98 forgetting factor.
Note: The figure presents the TCI obtained from using a forgetting factor of 0.98 in our main empirical model.

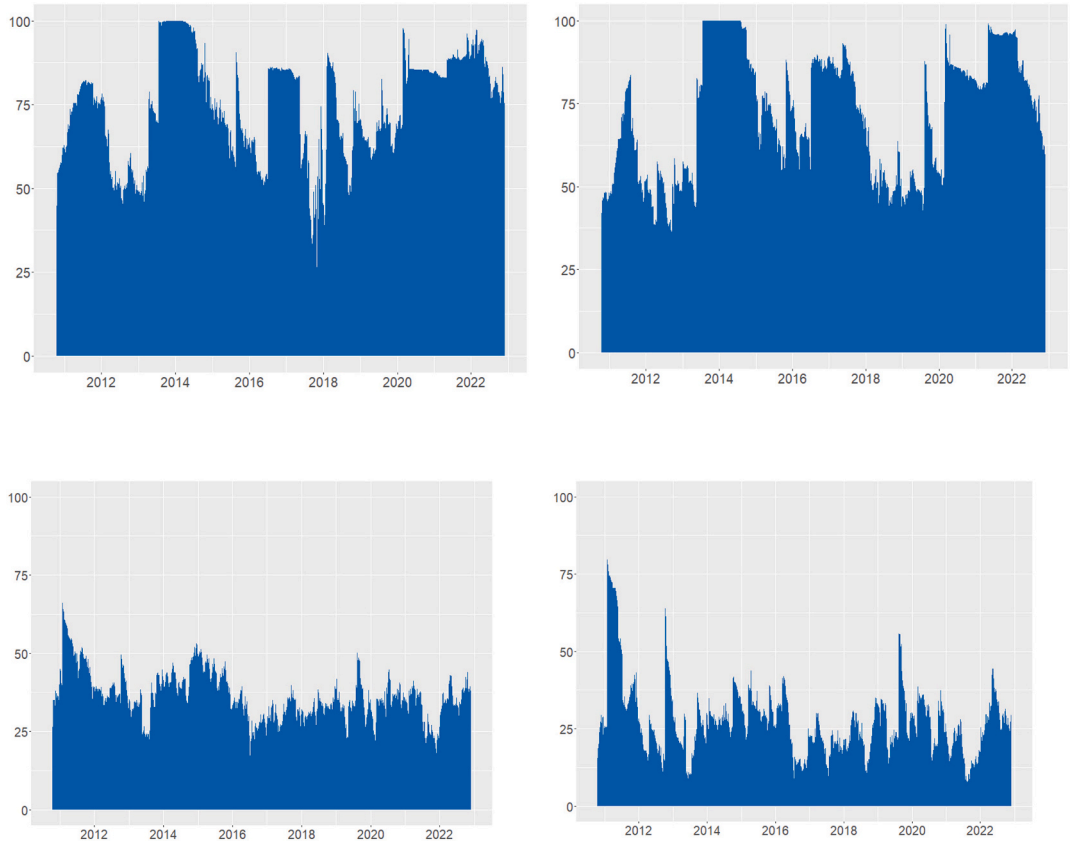

Fig. A.9. Total connectedness indexes – TVP-VAR Extended Joint Connectedness Model with a 0.97 forgetting factor.
Note: The figure presents the TCI obtained from using a forgetting factor of 0.97 in our main empirical model.

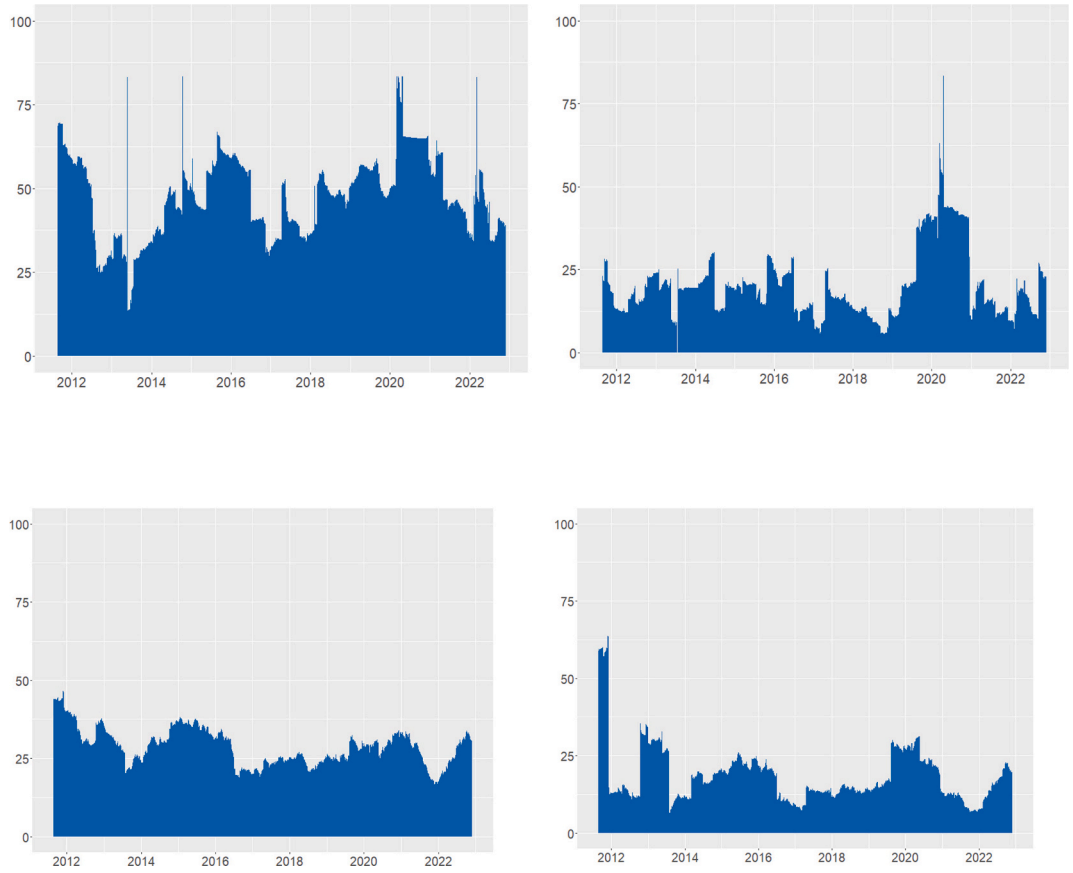

Fig. A.10. Original DY model with 200 days rolling window.
Note: The figure presents the TCI obtained from the Original DY Connectedness model with a 200-day rolling window.

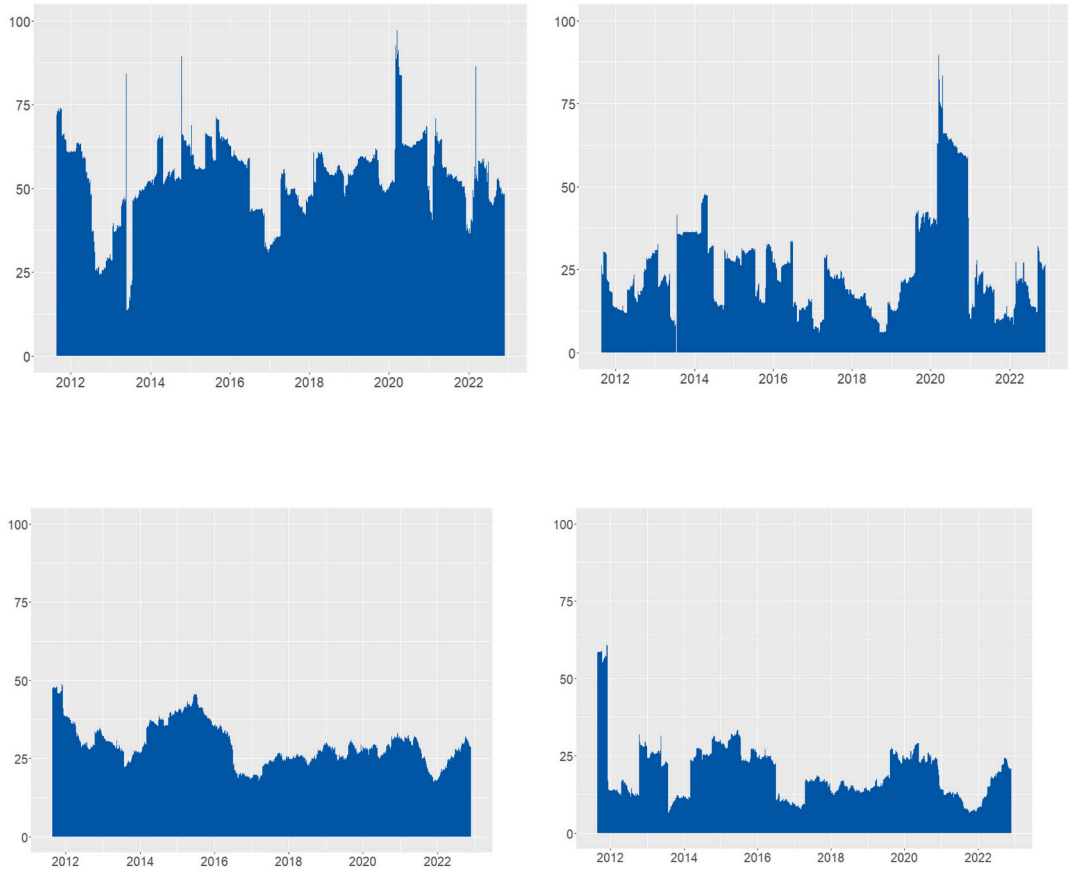

Fig. A.11. Extended Joint Connectedness model with a 200-day rolling window.
Note: The figure presents the TCI obtained from the Extended Joint Connectedness model with a 200-day rolling window.

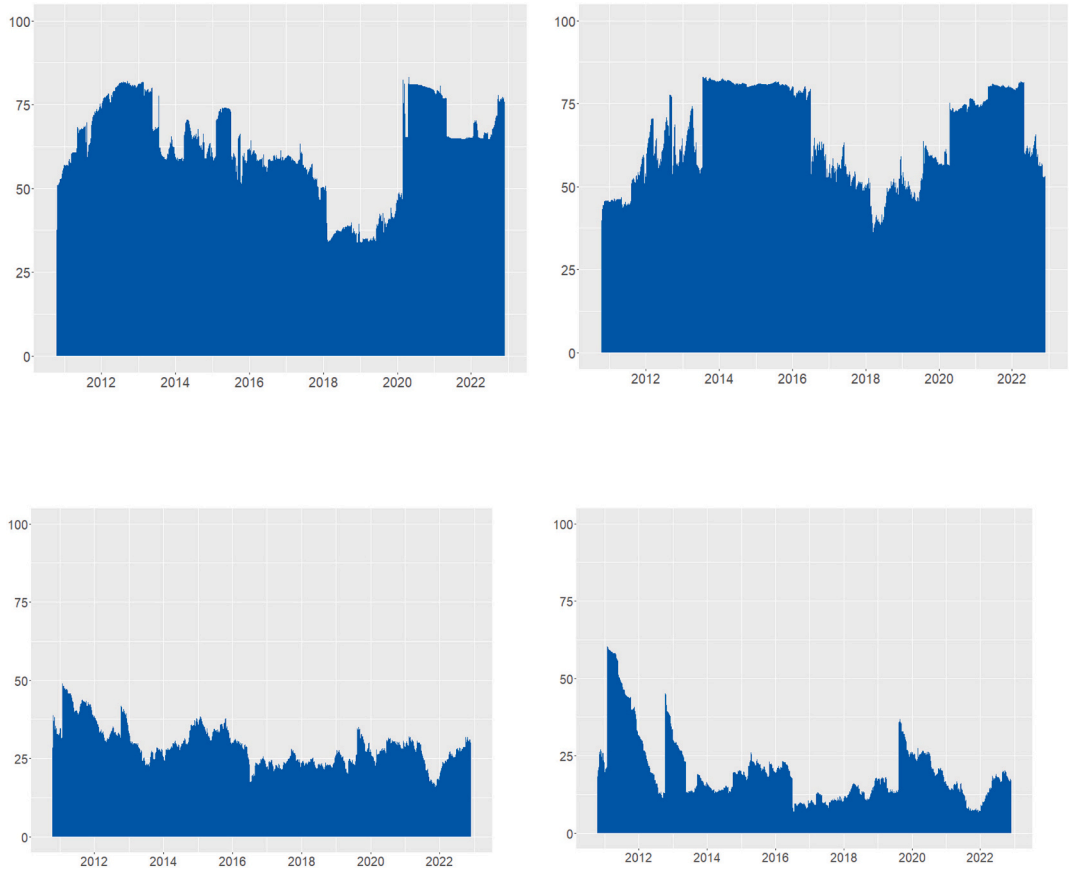

Fig. A.12. TVP-VAR Connectedness model.
Note: The figure presents the TCI obtained from the TVP-VAR model.

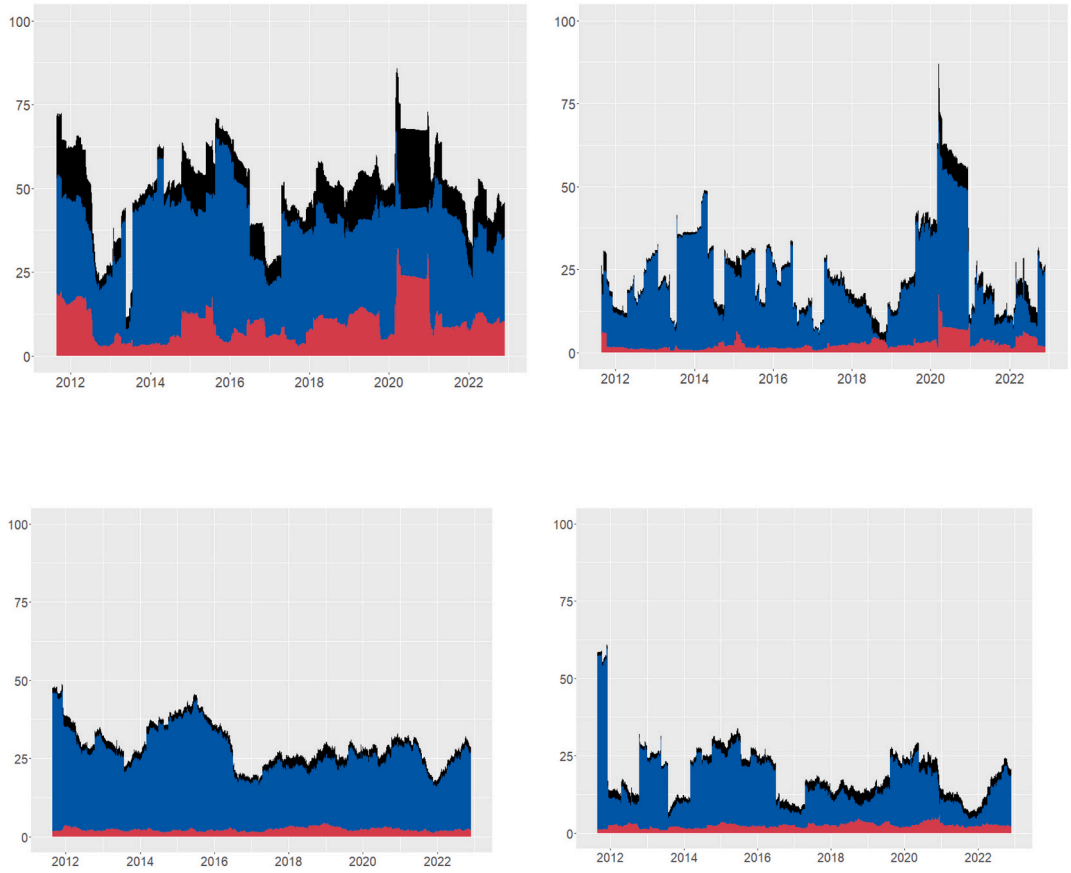

Fig. A.13. R2 Model-Free Connectedness model.
Note: The figure presents the TCI obtained from the R2 Model Free Connectedness. The black area represents total connectedness, while the blue and red areas represent the contemporaneous and lagged connectedness.

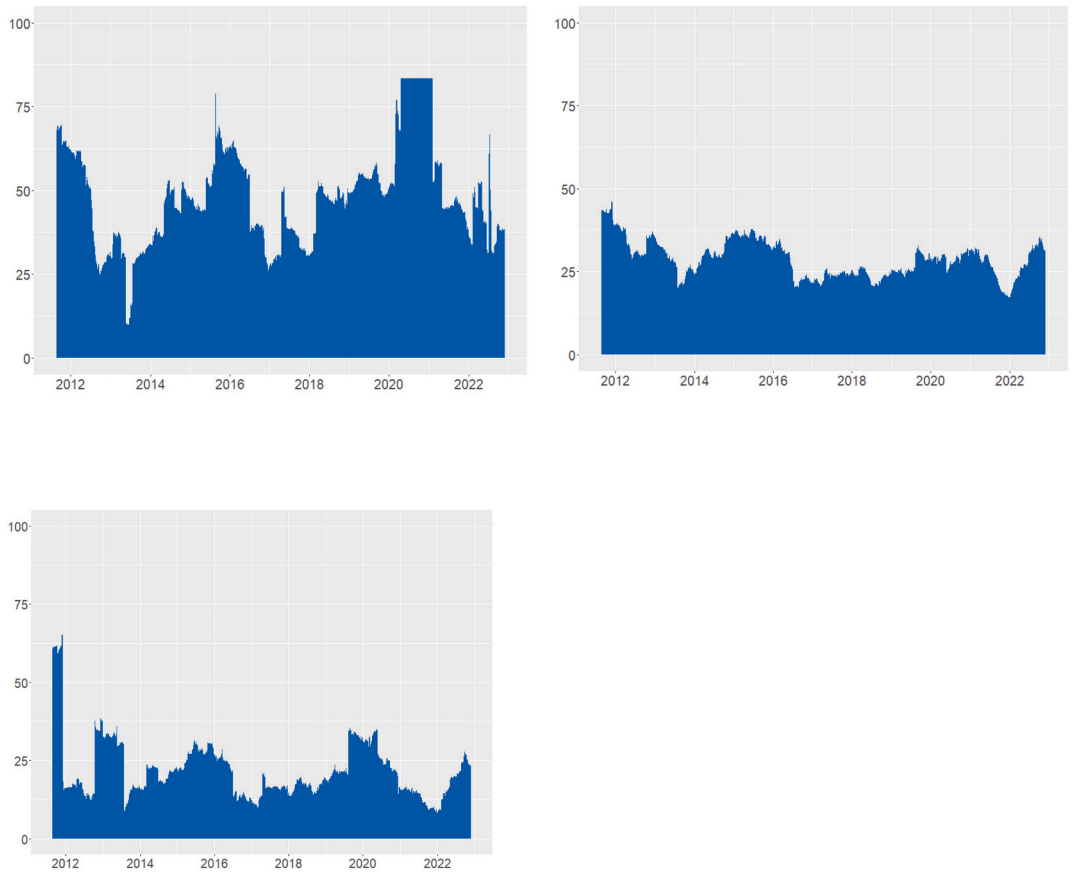

Fig. A.14. Quantile Connectedness model – Median quantile.
Note: The figure presents the TCI obtained from the Quantile Connectedness Model at the median quantile.

Appendix B. Robustness checks for the utility-based hedging portfolio performance

Table B.1
Expected utility gain under alternative hedging strategies – Post-COVID-19 period.

		Hedging strategies	
Portfolio	λ	Minimum Variance	Exponential Utility
(OIL, BIO)	10	−1.0838	0.2013
	5	−8.3189	0.2418
	10	−0.0096	0.1796
(OIL, SOLAR)	5	−0.0927	0.1686
	10	−0.7115	0.1685
(OIL, WIND)	5	−5.2968	0.1463
	10	−0.0858	0.1135
(OIL, REG)	5	−0.7337	0.0892
	10	−7.9299	1.1316
(OIL, ENEF)	5	−60.9713	2.1671

Note: The table presents the expected utility gain of the minimum variance hedge ratios and the exponential utility hedge ratios, compared to the utility of an unhedged position in oil, across different risk aversion parameters (λ) during the post-COVID-19 period from January 1, 2020 to the end of our sampling period. BIO, SOLAR, WIND, REG, and ENEF represent the NASDAQ OMX Biofuel, Wind, Solar, Renewable Energy Generation, and Energy Efficiency Indexes.

Table B.2
Expected utility gain under alternative utility-based hedging strategies – Full sample.

		Utility functions				
Portfolio	λ	Quadratic	Exponential Utility	Quartic	Power	Logarithm
(OIL, BIO)	10	0.1816	0.4039	1.5461	0.3982	0.2371
	5	0.3582	0.6706	1.7186	0.6876	0.4696
	10	1.1097	0.7490	2.5296	0.7434	0.4445
(OIL, SOLAR)	5	2.1850	1.2865	3.1536	1.3194	0.8871

(*continued on next page*)

Table B.2 (*continued*)

		Utility functions				
Portfolio	λ	Quadratic	Exponential Utility	Quartic	Power	Logarithm
(OIL, WIND)	10	0.9149	0.1463	1.4867	0.1253	0.0424
	5	1.8019	0.1198	0.8759	0.1104	0.0546
	10	0.4140	0.2430	1.5705	0.2281	0.1142
(OIL, REG)	5	0.8153	0.3363	1.2373	0.3366	0.2094
	10	0.3067	0.7067	2.0831	0.7173	0.4380
(OIL, ENEF)	5	0.6052	1.2904	2.7925	1.3277	0.8747

Note: The table presents the expected utility gain of hedging strategies based on the quadratic, cubic, quartic, power, and logarithm utility functions, compared to the utility of an unhedged position in oil, across different risk aversion parameters (λ). BIO, SOLAR, WIND, REG, and ENEF represent the NASDAQ OMX Biofuel, Wind, Solar, Renewable Energy Generation, and Energy Efficiency Indexes.

Table B.3
Expected utility gain under alternative utility-based hedging strategies – Post-COVID-19 period.

		Utility functions				
Portfolio	λ	Quadratic	Exponential Utility	Quartic	Power	Logarithm
(OIL, BIO)	10	0.1815	0.2013	1.2603	0.1875	0.0838
	5	0.3571	0.2418	0.9898	0.2355	0.1447
	10	1.0976	0.1796	1.3786	0.1584	0.0637
(OIL, SOLAR)	5	2.0875	0.1686	0.9036	0.1589	0.0822
	10	0.9151	0.1685	1.7053	0.1452	0.0488
(OIL, WIND)	5	1.8037	0.1463	1.0321	0.1364	0.0659
	10	0.4143	0.1135	1.1965	0.0963	0.0298
(OIL, REG)	5	0.8175	0.0892	0.6926	0.0807	0.0388
	10	0.3068	1.1316	2.3205	1.1662	0.7314
(OIL, ENEF)	5	0.6055	2.1671	4.1172	2.2369	1.4742

Note: The table presents the expected utility gain of hedging strategies based on the quadratic, cubic, quartic, power, and logarithm utility functions, compared to the utility of an unhedged position in oil, across different risk aversion parameters (λ) during the post COVID-19 period from January 1, 2020 to the end of our sampling period. BIO, SOLAR, WIND, REG, and ENEF represent the NASDAQ OMX Biofuel, Wind, Solar, Renewable Energy Generation, and Energy Efficiency Indexes.

Appendix C. Robustness checks for the minimum connectedness portfolio performance

Table C.1
Minimum connectedness portfolio performance indicators – Post-COVID 19 period

Table C.1.1. Portfolio return summary statistics

Portfolio	Mean Return	SD of Return	Info. Ratio
Oil (Unhedged)	0.00926	0.13781	0.06719
MCP (Realized Volatility)	0.00961	0.11938	0.08049
MCP (Jump component of realized volatility)	0.00431	0.06000	0.07177
MCP (Realized Skewness)	0.02354	0.03608	0.06523
MCP (Realized Kurtosis)	0.02331	0.03483	0.06691

Table C.1.2. Average weights of oil and hedging effectiveness

Portfolio	Mean weight	SD of weight	Hedging effectiveness (%)
Oil (Unhedged)	1.00	0.00	0.00
MCP (Realized Volatility)	0.50	0.26	0.25
MCP (Jump component of realized volatility)	0.19	0.20	0.81
MCP (Realized Skewness)	0.20	0.02	0.93
MCP (Realized Kurtosis)	0.19	0.01	0.94

Note: The table presents the performance indicators of an unhedged position in oil price and the minimum connectedness portfolio in realized volatility, the jump component of volatility, realized skewness, and realized kurtosis in the post-COVID-19 period from January 1, 2020 to the end of our sampling period. Table C.1.1 presents the portfolio returns, the standard deviation of returns, and the information ratios. Table C.1.2 reports the average weight of oil in each portfolio and the hedging effectiveness provided by each portfolio against variations in oil prices.

Table C.2
Minimum higher-moment connectedness portfolio performance indicators – Out-of-sample analysis.

Table C.2.1. Portfolio return summary statistics

Portfolio	Mean Return	SD of Return	Info. Ratio
Oil (Unhedged)	0.00322	0.08550	0.037758
MCP (Realized Volatility)	0.00303	0.07303	0.041555
MCP (Jump component of realized volatility)	0.00159	0.02893	0.055236
MCP (Realized Skewness)	0.00104	0.02341	0.044757
MCP (Realized Kurtosis)	0.00106	0.02242	0.047439

Table C.2.2. Average weights of oil and hedging effectiveness

Portfolio	Mean weight	SD of weight	Hedging effectiveness (%)
Oil (Unhedged)	1.00	0.00	0.00
MCP (Realized Volatility)	0.25	0.20	0.27
MCP (Jump component of realized volatility)	0.21	0.22	0.89
MCP (Realized Skewness)	0.22	0.04	0.93
MCP (Realized Kurtosis)	0.19	0.03	0.93

Note: The table presents the out-of-sample performance indicators of an unhedged position in oil price and the minimum connectedness portfolio in realized volatility, the jump component of volatility, realized skewness, and realized kurtosis. Table C.2.1 presents the portfolio returns, the standard deviation of returns, and the information ratios. Table C.2.2 reports the average weight of oil in each portfolio and the hedging effectiveness provided by each portfolio against variations in oil prices.

Table C.3
Minimum quantile connectedness portfolio performance indicators – Out-of-sample analysis.

Table C.3.1. Portfolio return summary statistics

Portfolio	Mean Return	SD of Return	Info. Ratio
Oil (Unhedged)	0.00322	0.08550	0.037758
MCP (Lower quantile)	0.00185	0.03700	0.05009
MCP (Upper quantile)	0.00130	0.03136	0.04156

Table C.3.2. Average weights of oil and hedging effectiveness

Portfolio	Mean weight	SD of weight	Hedging effectiveness (%)
Oil (Unhedged)	1.00	0.00	0.00
MCP (Lower quantile)	0.28	0.11	0.81
MCP (Upper quantile)	0.21	0.11	0.87

Note: The table presents the out-of-sample performance indicators of an unhedged position in oil price, and the minimum connectedness portfolio in the extreme lower and upper quantiles of returns (i.e., the 5th and 95th quantiles of returns). Table C.3.1 presents the portfolio returns, the standard deviation of returns, and the information ratios. Table C.3.2 reports the average weight of oil in each portfolio and the hedging effectiveness provided by each portfolio against variations in oil prices

Appendix D. Block diagram of methodology

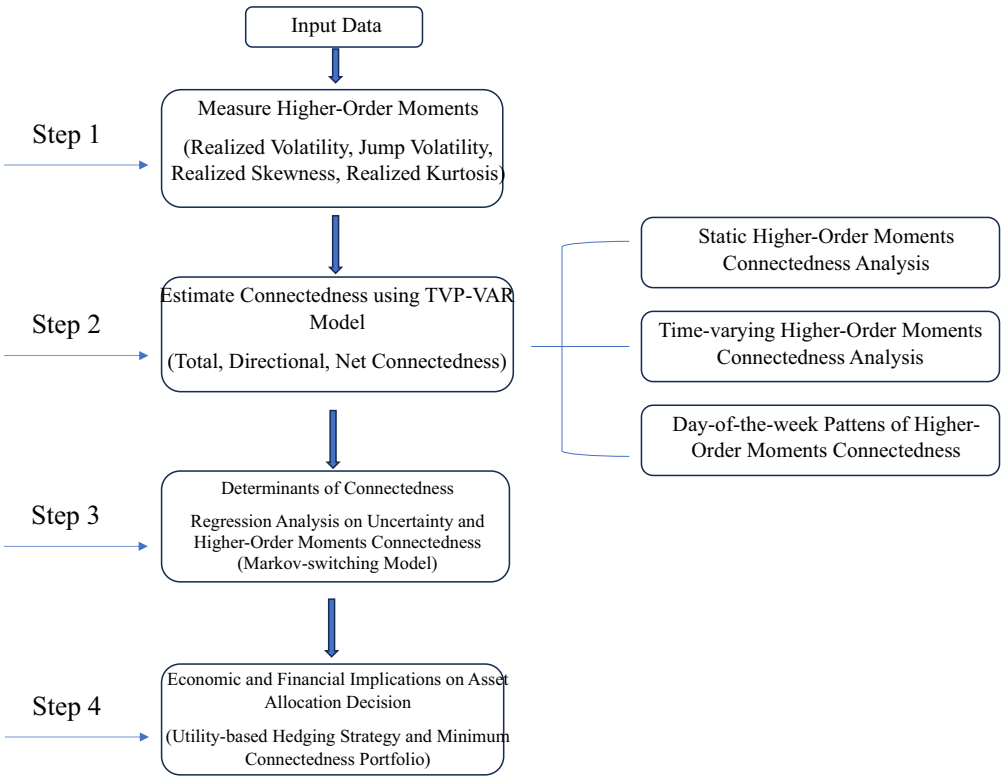

Appendix E. Supplementary data

Supplementary data to this article can be found online at https://doi.org/10.1016/j.eneco.2024.107987.

References

Ahmad, W., 2017. On the dynamic dependence and investment performance of crude oil and clean energy stocks. Res. Int. Bus. Financ. 42, 376–389.
Ahmad, W., Sadorsky, P., Sharma, A., 2018. Optimal hedge ratios for clean energy equities. Econ. Model. 72, 278–295.
Alexander, C., Barbosa, A., 2008. Hedging index exchange traded funds. J. Bank. Financ. 32 (2), 326–337.
Andersen, T.G., Bollerslev, T., 1998. Answering the skeptics: yes, standard volatility models do provide accurate forecasts. Int. Econ. Rev. 39, 885–905.
Andersen, T.G., Bollerslev, T., Diebold, F.X., Labys, P., 2003. Modeling and forecasting realized volatility. Econometrica 71 (2), 579–625.
Ando, T., Greenwood-Nimmo, M., Shin, Y., 2022. Quantile connectedness: modeling tail behavior in the topology of financial networks. Manag. Sci. 68 (4), 2401–2431.
Antonakakis, N., Chatziantoniou, I., Gabauer, D., 2020. Refined measures of dynamic connectedness based on time-varying parameter vector autoregressions. J. Risk Financ. Manag. 13 (4), 84.
Bakas, D., Triantafyllou, A., 2018. The impact of uncertainty shocks on the volatility of commodity prices. J. Int. Money Financ. 87, 96–111.
Balcilar, M., Gabauer, D., Umar, Z., 2021. Crude oil futures contracts and commodity markets: new evidence from a TVP-VAR extended joint connectedness approach. Res. Policy 73, 102219.
Balli, F., Balli, H.O., Dang, T.H.N., Gabauer, D., 2023. Contemporaneous and lagged R2 decomposed connectedness approach: new evidence from the energy futures market. Financ. Res. Lett. 57, 104168.
Barndorff-Nielsen, O.E., Kinnebrouk, S., Shephard, N., 2010. Measuring downside risk: Realised semivariance. In: Bollerslev, T., Russell, J., Watson, M. (Eds.), Volatility and Time Series Econometrics: Essays in Honor of Robert F. Engle. Oxford University Press, pp. 117–136.
Baruník, J., Kočenda, E., Vácha, L., 2015. Volatility spillovers across petroleum markets. Energy J. 36 (3), 309–329.
Baruník, J., Kočenda, E., Vácha, L., 2017. Asymmetric volatility connectedness on the forex market. J. Int. Money Financ. 77, 39–56.
Bloomberg New Energy Finance, 2023. Energy transition investment trends 2023. In: Technical Report.
Bonato, M., Gupta, R., Lau, C.K.M., Wang, S., 2020. Moments-based spillovers across gold and oil markets. Energy Econ. 89, 104799.
Bouri, E., Lei, X., Jalkh, N., Xu, Y., Zhang, H., 2021. Spillovers in higher moments and jumps across U.S. stock and strategic commodity markets. Res. Policy 72, 102060.
Broadstock, D.C., Cao, H., Zhang, D., 2012. Oil shocks and their impact on energy related stocks in China. Energy Econ. 34 (6), 1888–1895.
Broadstock, D.C., Chatziantoniou, I., Gabauer, D., 2022. Minimum connectedness portfolios and the market for green bonds: Advocating socially responsible investment (SRI) activity. In: Applications in Energy Finance: The Energy Sector, Economic Activity, Financial Markets and the Environment. Springer International Publishing, Cham, pp. 217–253.
Brooks, C., Černý, A., Miffre, J., 2012. Optimal hedging with higher moments. J. Futur. Mark. 32 (10), 909–944.
Corsi, F., Pirino, D., Renò, R., 2010. Threshold bipower variation and the impact of jump on volatility forecasting. J. Econ. 159 (2), 276–288.
Cotter, J., Hanly, J., 2015. Performance of utility based hedges. Energy Econ. 49, 718–726.
Cross, F., 1973. The behavior of stock prices on Fridays and Mondays. Financ. Anal. J. 29 (6), 67–69.
Dickey, D.A., Fuller, W.A., 1979. Distribution of the estimators for autoregressive time series with a unit root. Journal of the American Statistical Association 74 (366a), 427–431.
Diebold, F.X., Yilmaz, K., 2009. Measuring financial asset return and volatility spillovers, with application to global equity markets. Econ. J. 119 (534), 158–171.
Diebold, F.X., Yilmaz, K., 2012. Better to give than to receive: predictive directional measurement of volatility spillovers. Int. J. Forecast. 28 (1), 57–66.
Diebold, F.X., Yilmaz, K., 2014. On the network topology of variance decompositions: measuring the connectedness of financial firms. J. Econ. 182 (1), 119–134.
Ferrer, R., Shahzad, S.J.H., López, R., Jareño, F., 2018. Time and frequency dynamics of connectedness between renewable energy stocks and crude oil prices. Energy Econ. 76, 1–20.
Foglia, M., Angelini, E., Huynh, T.L.D., 2022. Tail risk connectedness in clean energy and oil financial market. Ann. Oper. Res. 334, 575–599.

Frank, M.Z., Sanati, A., 2018. How does the stock market absorb shocks? J. Financ. Econ. 129 (1), 136–153.
French, K.R., 1980. Stock returns and the weekend effect. J. Financ. Econ. 8 (1), 55–69.
Gkillas, K., Bouri, E., Gupta, R., Roubaud, D., 2022. Spillovers in higher-order moments of crude oil, gold, and bitcoin. Q. Rev. Econ. Finance 84, 398–406.
Gu, X., Zhu, Z., Yu, M., 2021. The macro effects of GPR and EPU indexes over the global oil market - are the two types of uncertainty shock alike? Energy Econ. 100, 105394.
Hammoudeh, S., Mokni, K., Ben-Salha, O., Ajmi, A.N., 2021. Distributional predictability between oil prices and renewable energy stocks: is there a role for the COVID-19 pandemic? Energy Econ. 103, 105512.
Hanif, W., Ko, H.E., Pham, L., Kang, S.H., 2023. Dynamic connectedness and network in the high moments of cryptocurrency, stock, and commodity markets. Financ. Innov. 9 (1), 1–40.
Henriques, I., Sadorsky, P., 2008. Oil prices and the stock prices of alternative energy companies. Energy Econ. 30 (3), 998–1010.
Hong, H., Lim, T., Stein, J.C., 2000. Bad news travels slowly: size, analyst coverage, and the profitability of momentum strategies. J. Financ. 55 (1), 265–295.
Kocaarslan, B., Soytas, U., 2019. Dynamic correlations between oil prices and the stock prices of clean energy and technology firms: the role of reserve currency (U.S. dollar). Energy Econ. 84, 104502.
Kumar, S., Managi, S., Matsuda, A., 2012. Stock prices of clean energy firms, oil and carbon markets: a vector autoregressive analysis. Energy Econ. 34 (1), 215–226.
Lastrapes, W.D., Wiesen, T.F., 2021. The joint spillover index. Econ. Model. 94, 681–691.
Lv, X., Dong, X., Dong, W., 2021. Oil prices and stock prices of clean energy: new evidence from Chinese subsectoral data. Emerg. Mark. Financ. Trade 57 (4), 1088–1102.
Lyu, Y., Tuo, S., Wei, Y., Yang, M., 2021. Time-varying effects of global economic policy uncertainty shocks on oil price volatility: new evidence. Res. Policy 70, 101943.
Managi, S., Okimoto, T., 2013. Does the price of oil interact with clean energy prices in the stock market? Jpn. World Econ. 27, 1–9.
Mitchell, M.L., Mulherin, J.H., 1994. The impact of public information on the stock market. J. Financ. 49 (3), 923–950.
Naeem, M.A., Peng, Z., Suleman, M.T., Nepal, R., Shahzad, S.J.H., 2020. Time and frequency connectedness among oil shocks, electricity and clean energy markets. Energy Econ. 91, 104914.
Nasreen, S., Tiwari, A.K., Eizaguirre, J.C., Wohar, M.E., 2020. Dynamic connectedness between oil prices and stock returns of clean energy and technology companies. J. Clean. Prod. 260, 121015.
Nekhili, R., Bouri, E., 2023. Higher-order moments and co-moments' contribution to spillover analysis and portfolio risk management. Energy Econ. 119, 10659.
Patton, A.J., 2004. On the out-of-sample importance of skewness and asymmetric dependence for asset allocation. J. Financ. Econ. 2 (1), 130–168.
Pham, L., 2019. Do all clean energy stocks respond homogeneously to oil price? Energy Econ. 81, 355–379.
Reboredo, J.C., 2015. Is there dependence and systemic risk between oil and renewable energy stock prices? Energy Econ. 48, 32–45.
Reboredo, J.C., Ugolini, A., 2016. Quantile dependence of oil price movements and stock returns. Energy Econ. 54, 33–49.
Sadorsky, P., 2012. Correlations and volatility spillovers between oil prices and the stock prices of clean energy and technology companies. Energy Econ. 34 (1), 248–255.
Saeed, T., Bouri, E., Alsulami, H., 2021. Extreme return connectedness and its determinants between clean/green and dirty energy investments. Energy Econ. 96, 105017.
Sukcharoen, K., Zohrabyan, T., Leatham, D., Wu, X., 2014. Interdependence of oil prices and stock market indices: a copula approach. Energy Econ. 44, 331–339.
Tiwari, A.K., Nasreen, S., Hammoudeh, S., Selmi, R., 2021. Dynamic dependence of oil, clean energy and the role of technology companies: new evidence from copulas with regime switching. Energy 220, 119590.
Tiwari, A.K., Abakah, E.J.A., Karikari, N.K., Hammoudeh, S., 2022. Time-varying dependence dynamics between international commodity prices and Australian industry stock returns: a perspective for portfolio diversification. Energy Econ. 108, 105891.
Tiwari, A.K., Trabelsi, N., Abakah, E.J.A., Nasreen, S., Lee, C.C., 2023. An empirical analysis of the dynamic relationship between clean and dirty energy markets. Energy Econ. 124, 106766.
Uddin, G.S., Rahman, M.L., Hedström, A., Ahmed, A., 2019. Cross-quantilogram-based correlation and dependence between renewable energy stock and other asset classes. Energy Econ. 80, 743–759.
Wang, X., Li, J., Ren, X., Bu, R., Jawadi, F., 2023. Economic policy uncertainty and dynamic correlations in energy markets: assessment and solutions. Energy Econ. 117, 106475.
Xia, T., Ji, Q., Zhang, D., Han, J., 2019. Asymmetric and extreme influence of energy price changes on renewable energy stock performance. J. Clean. Prod. 241, 118338.
Xiao, J., Zhou, M., Wen, F., Wen, F., 2018. Asymmetric impacts of oil price uncertainty on Chinese stock returns under different market conditions: evidence from oil volatility index. Energy Econ. 74, 777–786.
Yahya, M., Kanjilal, K., Dutta, A., Uddin, G.S., Ghosh, S., 2021. Can clean energy stock price rule oil price? New evidences from a regime-switching model at first and second moments. Energy Econ. 95, 105116.
Zhang, G., Liu, W., 2018. Analysis of the international propagation of contagion between oil and stock markets. Energy 165, 469–486.
Zhang, Y.J., Yan, X.X., 2020. The impact of U.S. economic policy uncertainty on WTI crude oil returns in different time and frequency domains. Int. Rev. Econ. Financ. 69, 750–768.
Zhang, H., Jin, C., Bouri, E., Gao, W., Xu, Y., 2023. Realized higher-order moments spillovers between commodity and stock markets: evidence from China. J. Commod. Mark. 30, 100275.